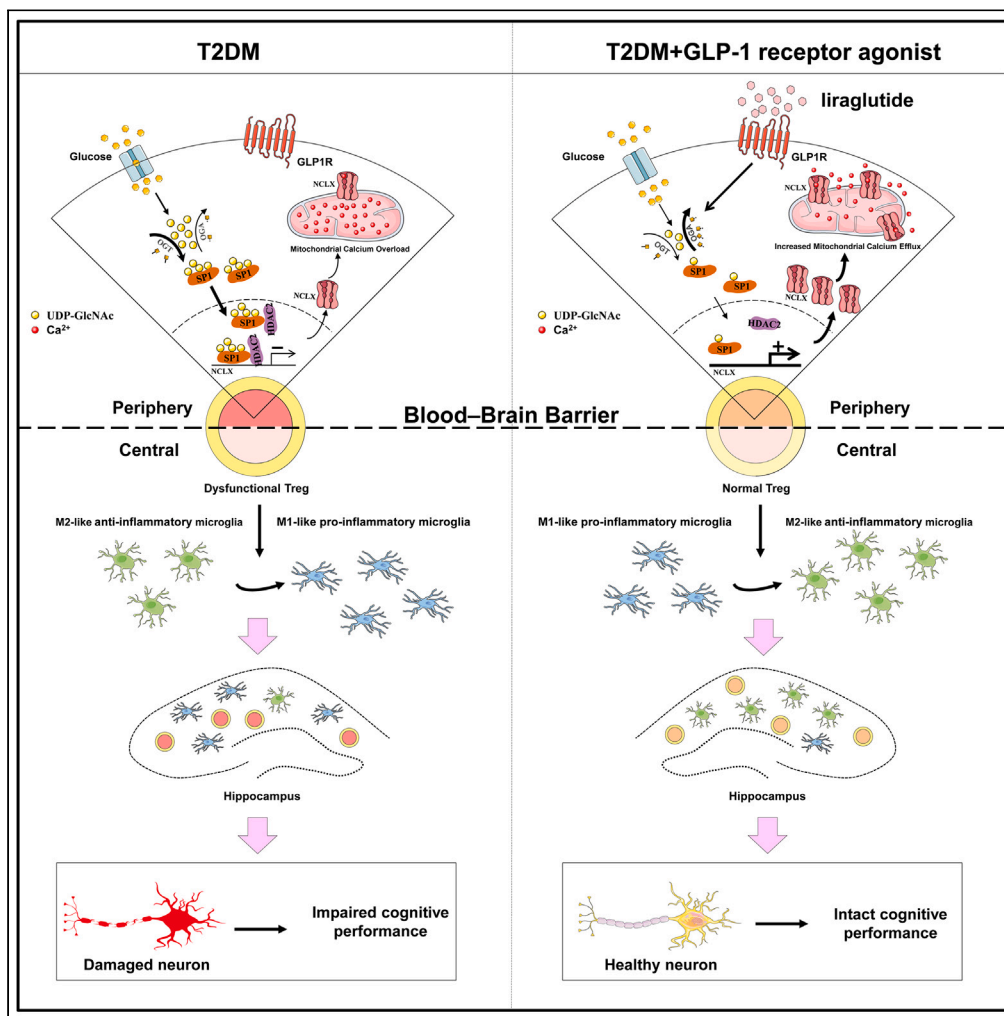


Article

High glucose impairs cognitive function through inducing mitochondrial calcium overload in Treg cells



Ya Hui, Liuyu Kuang, Yuanmei Zhong, Yunyun Tang, Zhiqiang Xu, Tianpeng Zheng

w19831120@126.com

Highlights
High glucose induces cognitive impairment by promoting Treg dysfunction

High glucose downregulates NCLX and leads to mitochondrial calcium overload in Treg

SP1 O-GlcNAcylation and HDAC2/NCLX signaling is involved in high-glucose-induced effects

GLP-1R agonist alleviates these effects via upregulation of OGA

Hui et al., iScience 27, 108689
January 19, 2024 © 2023 The Author(s).
<https://doi.org/10.1016/j.isci.2023.108689>



Article

High glucose impairs cognitive function through inducing mitochondrial calcium overload in Treg cells

Ya Hui,^{1,2,5,7} Liuyu Kuang,^{1,3,7} Yuanmei Zhong,^{1,4} Yunyun Tang,^{1,2} Zhiqiang Xu,¹ and Tianpeng Zheng^{1,2,3,4,6,8,*}

SUMMARY

High glucose has been proved to impair cognitive function in type 2 diabetes, but the underlying mechanisms remain elusive. Here, we found that high glucose increased transcription factors' SP1 O-GlcNAcylation in regulatory T (Treg) cells. Glycosylated SP1 further enhanced HDAC2 recruitment and histone deacetylation on Na⁺/Ca²⁺/Li⁺ exchanger (NCLX) promoter, which downregulated NCLX expression and led to mitochondrial calcium overload and oxidative damage, thereby promoting Treg cell dysfunction, M1 microglia polarization, and diabetes-associated cognitive impairment. Importantly, GLP-1 receptor agonist alleviated these deleterious effects via GLP-1-receptor-mediated upregulation of OGA and inhibition of SP1 O-GlcNAcylation in Treg cells. Our study highlighted a link between high-glucose-mediated SP1 O-GlcNAcylation and HDAC2/NCLX signaling in control of mitochondrial calcium concentrations in Treg cells. It also revealed a mechanism for linking Treg cell dysfunction and cognitive impairment in type 2 diabetes and provides an insight into the mechanism underlying the neuroprotective effects of GLP-1 receptor agonist.

INTRODUCTION

The risk of cognitive dysfunction was 1.5–2.0 times higher in patients with diabetes than in those without diabetes.¹ This relationship was independent of other risk factors for cognitive impairment and accounts for a prevalence rate varying between 13% and 24% in elderly diabetic patients.¹ Although hyperglycemia has been proved to promote the onset and development of cognitive impairment in type 2 diabetes, the underlying mechanisms are poorly defined. Regulatory T (Treg) cells, identified as the forkhead box protein P3 (Foxp3) + subset of CD4⁺ T cells, are known to play an essential role in curtailing excessive immune responses and preserving immune homeostasis.² Increasing evidence suggested that Treg cell dysfunction induced M1 microglia polarization, which further led to neuronal injury in neurodegenerative diseases.^{3,4} More importantly, recent studies demonstrated that high glucose conditions impaired the function and stability of Treg cells.^{5,6} However, the precise mechanism underlying these effects remains to be elucidated. In addition, whether and how high-glucose-induced Treg cell dysfunction contributes to cognitive impairment in type 2 diabetes is largely unknown.

Mitochondria are critical organelles for various cellular processes including oxidative phosphorylation, ATP production, reactive oxygen species generation, apoptosis induction, etc.⁷ Treg cells under steady-state conditions or upon activation had enhanced mitochondrial metabolism, with mitochondrial respiratory chain being vital for their stability, suppression capacity, and survival.⁸ Consistently, recent study by Alissafi et al. demonstrated that mitochondrial oxidative damage led to Treg cells defects in autoimmunity.⁸ It is generally acknowledged that mitochondrial calcium homeostasis is maintained in a coordinated fashion by regulators controlling calcium influx and efflux, and its disruption may lead to mitochondrial calcium overload and oxidative damage.^{9,10} Mitochondrial Na⁺/Ca²⁺/Li⁺ exchanger (NCLX), also known as solute carrier family 24 member 6 (SLC24A6), was identified as a crucial regulator responsible for mitochondrial calcium efflux.¹¹ NCLX plays a critical role in regulating mitochondrial and cytosolic Ca²⁺ signaling under high glucose conditions.¹² In addition, NCLX has emerged as a promising target for developing drugs against neurodegenerative diseases such as Alzheimer disease and Parkinson disease.¹³ Although previous studies suggested a crucial role of NCLX in maintaining mitochondrial calcium homeostasis, a complete understanding of whether and

¹Department of Endocrinology and Metabolism, The Second Affiliated Hospital of Guilin Medical University, Guilin, Guangxi 541199, P.R. China

²Guangxi Clinical Research Center for Diabetes and Metabolic Diseases, The Second Affiliated Hospital of Guilin Medical University, Guilin, Guangxi 541199, P.R. China

³Guangxi Key Laboratory of Diabetic Systems Medicine, Guilin Medical University, Guilin, Guangxi 541199, P.R. China

⁴Guangxi Key Laboratory of Metabolic Reprogramming and Intelligent Medical Engineering for Chronic Diseases, The Second Affiliated Hospital of Guilin Medical University, Guilin, Guangxi 541199, P.R. China

⁵Guangxi Key Laboratory of Brain and Cognitive Neuroscience, Guilin Medical University, Guilin, Guangxi 541199, P.R. China

⁶Guangxi Health Commission Key Laboratory of Glucose and Lipid Metabolism Disorders, The Second Affiliated Hospital of Guilin Medical University, Guilin, Guangxi 541199, P.R. China

⁷These authors contributed equally

⁸Lead contact

*Correspondence: w19831120@126.com

<https://doi.org/10.1016/j.isci.2023.108689>



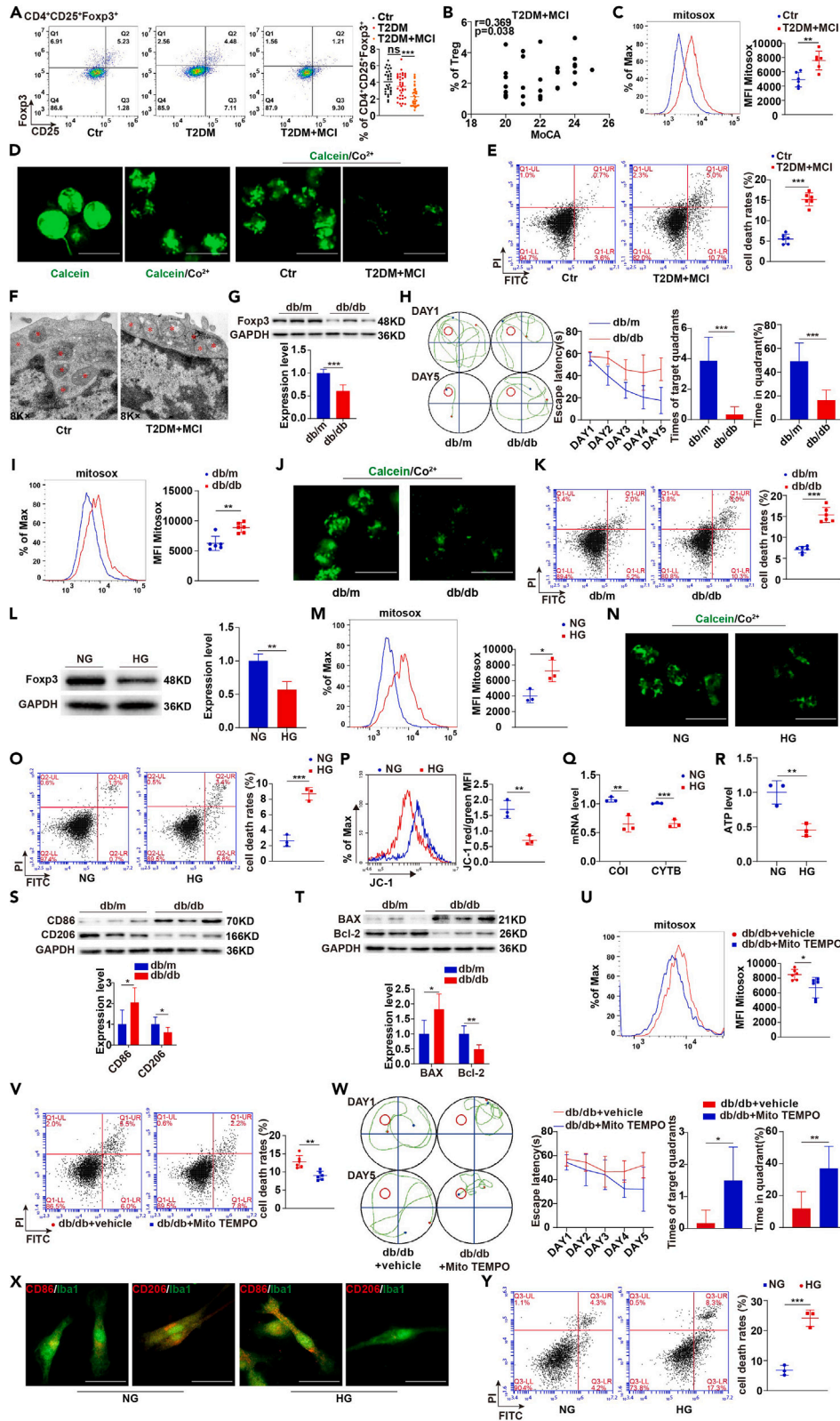


Figure 1. Hyperglycemia impairs Treg cell function through mitochondrial oxidative damage and induces M1 microglia polarization and cognitive impairment

- (A) Proportions of CD4⁺CD25⁺Foxp3⁺ Treg cells in the peripheral blood of control subjects, newly diagnosed type 2 diabetic patients without cognitive dysfunction, and type 2 diabetic patients with MCI were assessed by flow cytometry.
- (B) Correlation analysis of peripheral Treg cell frequencies with MoCA scores in type 2 diabetic patients with MCI.
- (C) Mean fluorescence intensity (MFI) of mtROS production measured by flow cytometry using MitoSox Red in Treg cells isolated from control subjects and type 2 diabetic patients with MCI.
- (D) Monitoring the opening of MPTP in Treg cells isolated from control subjects and type 2 diabetic patients with MCI. Cells were loaded with calcein-AM in the presence of Co²⁺.
- (E) Flow cytometry analysis of apoptosis in Treg cells isolated from control subjects and type 2 diabetic patients with MCI. Quantitative data show percentage of cell death rates.
- (F) Representative transmission electron microscope (TEM) images of the mitochondrial morphology in Treg cells isolated from control subjects and type 2 diabetic patients with MCI. The red asterisks indicate mitochondria.
- (G) Immunoblots and quantification analysis of protein level of Foxp3 in the hippocampus of db/m and db/db mice.
- (H) Morris water maze behavioral assessment for db/m and db/db mice showing differences in path (left), escape latency (second from left), number of times mice passed through the platform location in the probe trial (second from right), and the time mice stayed in the target quadrant (right) during learning session.
- (I–K) mtROS levels (I), MPTP opening (J), and apoptosis levels (K) in Treg cells isolated from db/m and db/db mice.
- (L–R) Immunoblots and quantification analysis of protein level of Foxp3 (L), mtROS levels (M), MPTP opening (N), apoptosis levels (O), MMP (P), mRNA levels of mitochondrial functional genes COI, CYTB (Q), and ATP levels (R) in human Treg cells treated with normal glucose (NG, 5.5 mmol/L D-glucose) or high glucose (HG, 25 mmol/L D-glucose) for 72 h.
- (S and T) Immunoblots and quantification analysis of protein levels of CD86, CD206 (S) and BAX, Bcl-2 (T) in the hippocampus of db/m and db/db mice.
- (U and V) mtROS levels (U) and apoptosis levels (V) in Treg cells isolated from db/db + vehicle and db/db + Mito TEMPO mice.
- (W) Morris water maze behavioral assessment for db/db + vehicle and db/db + Mito TEMPO mice showing differences in path (left), escape latency (second from left), number of times mice passed through the platform location in the probe trial (second from right), and the time mice stayed in the target quadrant (right) during learning session.
- (X) Representative images for CD86 and CD206 in microglia cocultured with normal glucose (NG, 5.5 mmol/L D-glucose) or high-glucose (HG, 25 mmol/L D-glucose)-treated Treg cells.
- (Y) Flow cytometry analysis of apoptosis in primary hippocampal neurons cocultured with microglia under different treatment. [Samples: (1) NG (5.5 mmol/L D-glucose), (2) HG (25 mmol/L D-glucose)]. Quantitative data show percentage of cell death rates.

how high glucose regulate NCLX expression in Treg cells is lacking; additionally, it remains unknown whether high glucose could induce mitochondrial oxidative damage by affecting NCLX function and subsequently lead to Treg cell dysfunction and cognitive impairment in type 2 diabetes.

In this study, we found that high glucose increased transcription factors' SP1 O-GlcNAcylation in Treg cells. Glycosylated SP1 further enhanced HDAC2 recruitment and histone deacetylation on NCLX promoter, which downregulated NCLX expression and led to mitochondrial calcium overload and oxidative damage, thereby promoting Treg cell dysfunction, M1 microglia polarization, and cognitive impairment in type 2 diabetes. Importantly, GLP-1 receptor agonist alleviated these deleterious effects in type 2 diabetes via GLP-1-receptor-mediated upregulation of OGA and inhibition of SP1 O-GlcNAcylation in Treg cells. These results provided a mechanistic view of how high glucose led to Treg cell dysfunction to initiate cognitive impairment in type 2 diabetes.

RESULTS**Hyperglycemia impairs Treg cell function through mitochondrial oxidative damage and induces M1 microglia polarization and cognitive impairment**

To investigate the relationship between Treg cell and cognitive impairment in type 2 diabetes, we first assessed CD4⁺CD25⁺Foxp3⁺ Treg frequencies in peripheral blood of 30 nondiabetic subjects, 36 newly diagnosed type 2 diabetic patients without cognitive dysfunction, and 34 diabetic patients with mild cognitive impairment (MCI). Detailed demographic and clinical data were listed in Table S1. After adjustment for BMI and SBP, our findings demonstrated a significant reduction of Treg frequencies in type 2 diabetic patients with MCI compared with nondiabetic control subjects and type 2 diabetic patients without MCI (Figure 1A), which was consistent with previous reports.^{5,14} In addition, we found a negative correlation between Treg frequencies and Montreal Cognitive Assessment (MoCA) scores in this group but not in newly diagnosed type 2 diabetes or control groups (Figures 1B, S1A, and S1B). Because mitochondrial dysfunction has been reported to exert a major impact on Treg function and even their survival,⁸ CD4⁺CD25⁺CD127⁻ Treg cells isolated from peripheral blood of nondiabetic control subjects and type 2 diabetic patients with MCI were subjected to mitochondrial function analysis. As shown in Figures 1C–1E and S1C–S1E, Treg cells isolated from type 2 diabetic patients with MCI exhibited increased mitochondrial reactive oxygen species (mtROS) production (Figure 1C), mitochondrial permeability transition pore (MPTP) opening (Figure 1D), and apoptosis (Figure 1E) compared with Treg cells isolated from nondiabetic control subjects, and these effects were accompanied by a decrease in mitochondrial membrane potential (MMP) (Figure S1C), mtDNA content (COI CYTB) (Figure S1D), and ATP productions (Figure S1E). Consistently, Treg cells isolated from type 2 diabetic patients with MCI displayed severely aberrant mitochondrial morphology characterized by swollen mitochondria with disorganized cristae (Figure 1F). Next, we used db/db mice as an animal model of type 2 diabetes to further validate these findings. As expected, our data confirmed that db/db mice had lower Foxp3 expression in the hippocampus (Figure 1G) and showed a significantly worse cognitive performance (Figures 1H and S1F) than db/m mice. In addition, CD4⁺CD25⁺ Treg cells were also isolated from their spleen and lymph nodes and

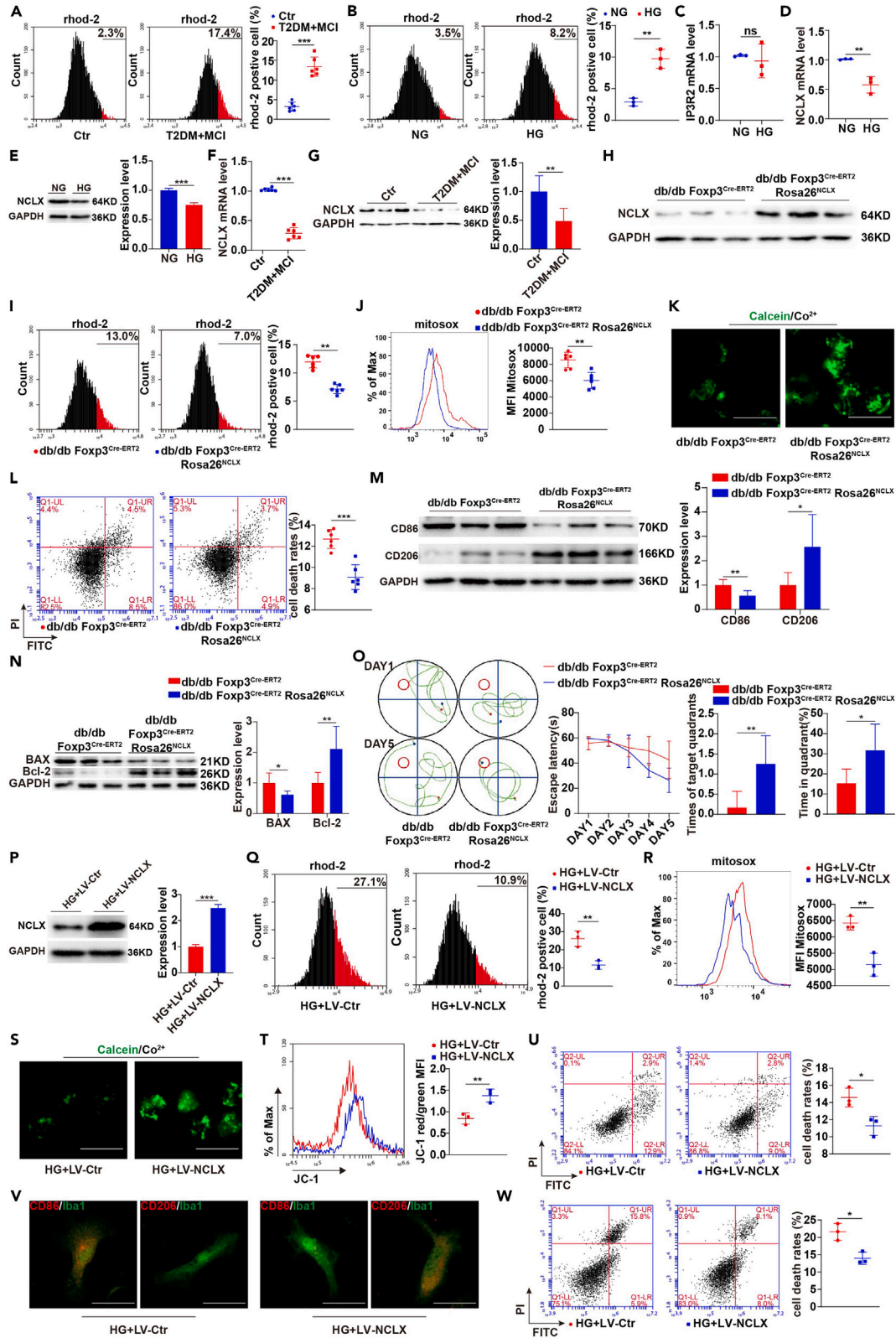


Figure 2. High glucose triggers mitochondrial oxidative damage by downregulating NCLX expression and inducing mitochondrial calcium overload in Treg cells

(A) Flow cytometry analysis using Rhod-2 revealed mitochondrial calcium levels in Treg cells isolated from control subjects and type 2 diabetic patients with MCI. Quantitative data show percentage of Rhod-2-positive cells.

(B) Flow cytometry analysis of mitochondrial calcium levels in human Treg cells treated with normal glucose (NG, 5.5 mmol/L D-glucose) or high glucose (HG, 25 mmol/L D-glucose) for 72 h. Quantitative data show percentage of Rhod-2-positive cells.

(C–E) mRNA levels of IP3R2 (C) and NCLX (D) and quantification analysis of protein level of NCLX (E) in human Treg cells treated with normal glucose (NG, 5.5 mmol/L D-glucose) or high glucose (HG, 25 mmol/L D-glucose) for 72 h.

(F and G) mRNA level of NCLX (F) and quantification analysis of protein level of NCLX (G) in Treg cells isolated from control subjects and type 2 diabetic patients with MCI.

(H–L) Immunoblot analysis of protein level of NCLX (H), flow cytometry analysis of mitochondrial calcium levels (I), mtROS levels (J), MPTP opening (K), and apoptosis levels (L) in Treg cells isolated from db/db Foxp3^{Cre-ERT2} and db/db Foxp3^{Cre-ERT2} Rosa26^{NCLX} mice.

(M and N) Immunoblots and quantification analysis of protein levels of CD86, CD206 (M) and BAX, Bcl-2 (N) in the hippocampus of db/db Foxp3^{Cre-ERT2} and db/db Foxp3^{Cre-ERT2} Rosa26^{NCLX} mice.

(O) Morris water maze behavioral assessment for db/db Foxp3^{Cre-ERT2} and db/db Foxp3^{Cre-ERT2} Rosa26^{NCLX} mice showing differences in path (left), escape latency (second from left), number of times mice passed through the platform location in the probe trial (second from right), and the time mice stayed in the target quadrant (right) during learning session.

(P–U) Immunoblots and quantification analysis of protein level of NCLX (P), flow cytometry analysis of mitochondrial calcium levels (Q), mtROS levels (R), MPTP opening (S), MMP (T), and apoptosis levels (U) in human Treg cells infected with NCLX-overexpressing lentivirus or control lentivirus in the presence of high glucose (HG, 25 mmol/L D-glucose).

(V) Representative images for CD86 and CD206 in microglia cocultured with high glucose (HG, 25 mmol/L D-glucose)-treated Treg cells in the presence of NCLX-overexpressing lentivirus or control lentivirus.

(W) Flow cytometry analysis of apoptosis in primary hippocampal neurons cocultured with microglia under different treatment. [Samples: (1) HG + LV-Ctr, (2) HG + LV-NCLX]. Quantitative data show percentage of cell death rates.

prepared for mitochondrial function analysis. As shown in Figures 1I–1K and S1G–S1I, db/db mice exhibited increased mtROS production (Figure 1I), MPTP opening (Figure 1J), and apoptosis (Figure 1K) but decreased MMP (Figure S1G), mtDNA content (Figure S1H), and ATP productions (Figure S1I) in their Treg cells as compared with db/m mice. Similar results were also obtained using high concentrations of glucose to treat *in vitro*-expanded human (Figures 1L–1R) and mice Tregs (Figures S1J–S1P), further confirming the role of hyperglycemia in the downregulation of Foxp3 and mitochondrial oxidative damage in Treg cells.

Because Treg cells have been proved to switch the microglia polarization from pro-inflammatory M1 phenotype to anti-inflammatory M2 phenotype and thereby exert protective effects on neurons,³ we asked whether hyperglycemia could polarize microglia toward a pro-inflammatory M1 phenotype and lead to cognitive defects by promoting mitochondrial oxidative damage in Treg cells. As shown in Figures 1S and 1T, db/db mice had higher CD86 (M1 microglia marker) and lower CD206 (M2 microglia marker) expression in the hippocampus than db/m mice (Figure 1S), and these effects were associated with an increased hippocampal neuron apoptosis (Figure 1T). To address the role of mitochondrial oxidative damage in hyperglycemia-induced Treg death, microglia polarization, and cognitive impairment, we further treated db/db mice with MitoTEMPO, a mitochondria-specific superoxide scavenger. As shown in Figures 1U and 1V, scavenging of mtROS significantly reduced mtROS production (Figure 1U) and diminished Treg cells apoptosis (Figure 1V) in db/db mice. These results were accompanied by improved cognitive function (Figures 1W and S1Q) and restoration of M2 microglia polarization as evidenced by increased CD206 and decreased CD86 expression in the hippocampus (Figure S1R). To confirm the *in vivo* findings mentioned earlier, we also performed experiments using a coculture system. Mice Treg cells were treated with or without high concentrations of glucose for 3 days and then cocultured with primary mouse microglia for another 3 days. Microglia cocultured with high-glucose-treated Treg cells displayed lower CD206 (M2 microglia marker) and higher CD86 (M1 microglia marker) expression (Figure 1X). Furthermore, hippocampal neurons cocultured with high-glucose-treated Treg-cell-conditioned microglia showed increased apoptosis compared with controls (Figure 1Y). In support, scavenging of mtROS in high-glucose-treated Treg cells restrained mtROS production and reduced Treg cell apoptosis (Figures S1S and S1T), thereby polarizing microglia toward an M2 phenotype and lowering hippocampal neuron death (Figures S1U and S1V). Overall, these findings indicate that hyperglycemia polarizes microglia toward a pro-inflammatory M1 phenotype and leads to cognitive impairment by inducing mitochondrial oxidative damage in Treg cells.

High glucose triggers mitochondrial oxidative damage by downregulating NCLX expression and inducing mitochondrial calcium overload in Treg cells

It is well established that mitochondrial calcium overload can result in mitochondrial oxidative damage.¹⁵ Thus, we tested whether high-glucose-mediated mitochondrial oxidative damage was associated with mitochondrial calcium overload in Treg cells. To this end, mitochondrial Ca²⁺ levels in human and mice Treg cells were measured by Rhod-2 probe (specific mitochondrial Ca²⁺ indicator) using flow cytometer. As shown in Figures 2A and S2A, Treg cells isolated from type 2 diabetic patients with MCI or db/db mice demonstrated increased mitochondrial calcium levels as compared with their respective controls. Similarly, mitochondrial calcium levels were increased in *in vitro*-expanded human and mice Treg cells treated with high glucose (Figures 2B and S2B). These results indicated that high glucose induced mitochondrial calcium overload in Treg cells.

IP3R2 and NCLX are two critical regulators that balance the mitochondrial calcium concentrations. IP3R2 is responsible for triggering calcium influx from the ER to mitochondria by interacting with Vdac1 to form an ER-mitochondria calcium tunnel.^{16,17} On the other hand, NCLX is

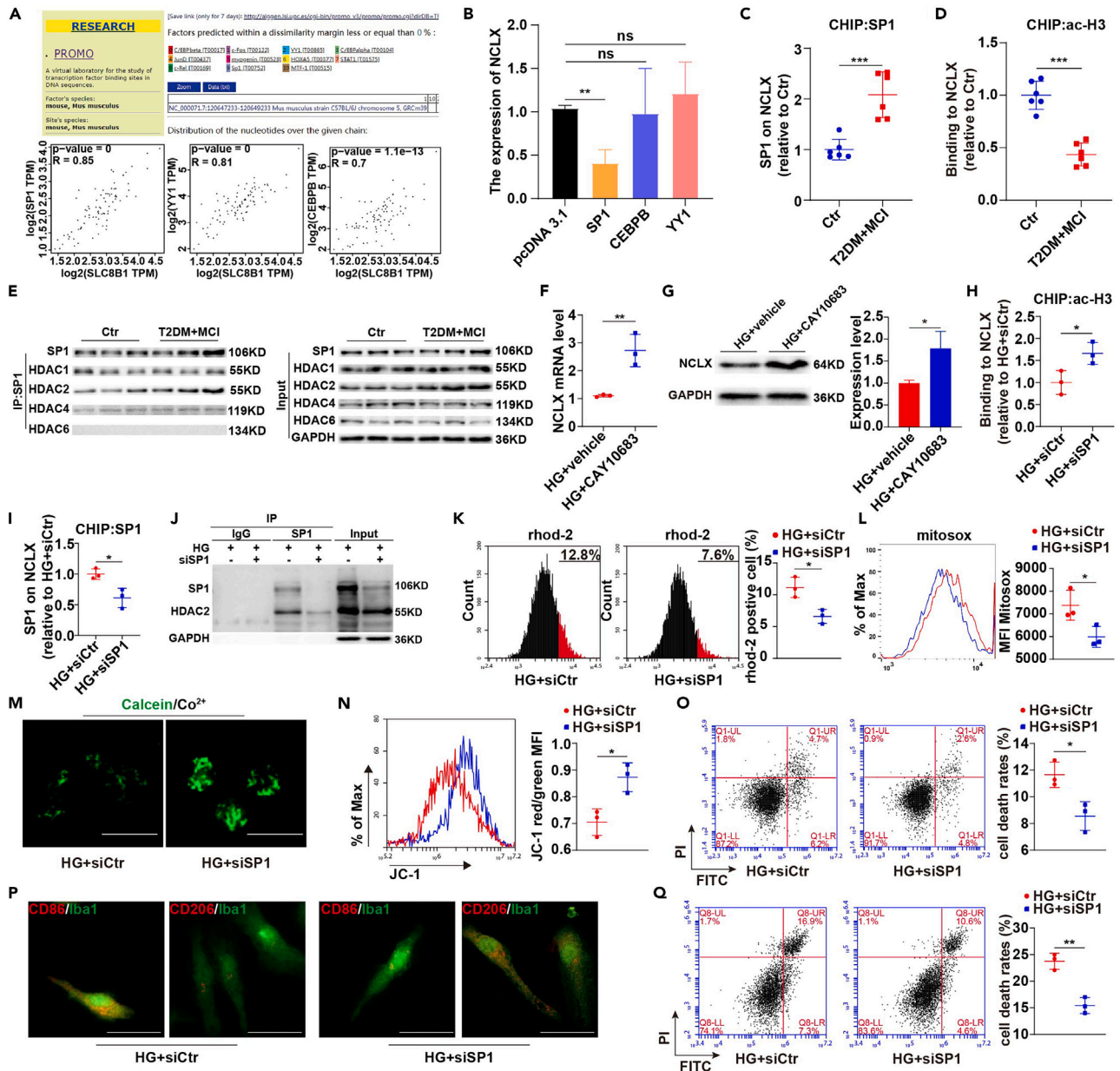


Figure 3. SP1-mediated HDAC2 recruitment and histone deacetylation lead to NCLX downregulation and Treg cell function impairment under high glucose conditions

(A) Identification of the transcription factors predicted to associate with the promoter of NCLX (SLC8B1), as determined by PROMO software. A total of 11 transcription factors were identified (upper panel). Correlation analysis of NCLX (SLC8B1) with SP1 (bottom left panel), YY1 (bottom middle panel), and CEBPB (bottom right panel).

(B) Relative expression of NCLX mRNA after SP1, CEBPB, or YY1 overexpression in human Treg cells, as detected by RT-PCR.

(C) Binding of SP1 to the NCLX promoter in Treg cells isolated from control subjects and type 2 diabetic patients with MCI.

(D) Levels of histone H3 lysine acetylation (ac-H3) on the NCLX promoter in Treg cells isolated from control subjects and type 2 diabetic patients with MCI.

(E) Treg cells isolated from control subjects and type 2 diabetic patients with MCI were used for IP assay with anti-SP1 antibodies and control normal IgG and analyzed using IB as indicated.

(F and G) mRNA level of NCLX (F) and quantification analysis of protein level of NCLX (G) in human Treg cells treated with or without HDAC inhibitor Santacruzamate A (CAY10683) in the presence of high glucose (HG, 25 mmol/L D-glucose).

(H) Levels of histone H3 lysine acetylation (ac-H3) on the NCLX promoter in human Treg cells treated with high glucose (HG, 25 mmol/L D-glucose) in the presence of control siRNA or SP1 siRNA for 72 h.

Figure 3. Continued

(I) Binding of SP1 to the NCLX promoter in human Treg cells treated with high glucose (HG, 25 mmol/L D-glucose) in the presence of control siRNA or SP1 siRNA for 72 h.

(J) Human Treg cells treated with control siRNA or SP1 siRNA in the presence of high glucose (HG, 25 mmol/L D-glucose) were used for IP assay with anti-SP1 antibodies and control normal IgG and analyzed using IB as indicated.

(K–O) Flow cytometry analysis of mitochondrial calcium levels (K), mtROS levels (L), MPTP opening (M), MMP (N), and apoptosis levels (O) in human Treg cells treated with SP1 siRNA or control siRNA in the presence of high glucose (HG, 25 mmol/L D-glucose).

(P) Representative images for CD86 and CD206 in microglia cocultured with high glucose (HG, 25 mmol/L D-glucose)-treated Treg cells in the presence of control siRNA or SP1 siRNA for 72 h.

(Q) Flow cytometry analysis of apoptosis in primary hippocampal neurons cocultured with microglia under different treatment. [Samples: (1) HG + siCtr, (2) HG + siSP1]. Quantitative data show percentage of cell death rates.

a mitochondrial sodium/calcium antiporter that mediates sodium-dependent calcium efflux from mitochondria.^{13,18} To explore the mechanism of how high glucose induces mitochondrial calcium overload in Treg cells, we examined whether IP3R2 or NCLX expression was affected by high glucose. There was no marked difference in IP3R2 mRNA levels between Treg cells treated with or without high glucose (Figures 2C and S2C). However, we found that high-glucose treatment reduced the gene and protein expression levels of NCLX in human and mice Treg cells (Figures 2D, 2E, S2D, and S2E). Consistently, NCLX gene and protein expression levels were also decreased in Tregs isolated from type 2 diabetic patients with MCI or db/db mice as compared with their respective controls (Figures 2F, 2G, S2F, and S2G). These results suggested that high glucose downregulated NCLX gene and protein expression in Treg cells.

To mechanistically link the high-glucose-mediated NCLX downregulation with mitochondrial calcium overload and oxidative damage in Tregs, we specifically overexpressed NCLX in Tregs by crossing Cre-inducible db/m mice carrying CAG-loxP-STOP-loxP-NCLX cassette at Rosa26 locus ($Rosa26^{NCLX}$) with $Foxp3^{Cre-ERT2}$ mice to generate db/db $Foxp3^{Cre-ERT2}$ $Rosa26^{NCLX}$ mice (Figure S2H). Tamoxifen-containing diet feeding successfully induced Treg-cell-specific overexpression of NCLX in db/db $Foxp3^{Cre-ERT2}$ $Rosa26^{NCLX}$ mice (Figures 2H and S2I). Remarkably, Treg cells isolated from db/db $Foxp3^{Cre-ERT2}$ $Rosa26^{NCLX}$ mice had reduced mitochondrial calcium levels than db/db $Foxp3^{Cre-ERT2}$ mice (Figure 2I), confirming that NCLX overexpression in Treg cells alleviated mitochondrial calcium overload in diabetes. Accordingly, NCLX overexpression improved mitochondrial dysfunction and reduced oxidative damage in Treg cells isolated from db/db $Foxp3^{Cre-ERT2}$ $Rosa26^{NCLX}$ mice (Figures 2J, 2K, and S2J). In addition, NCLX overexpression diminished Treg apoptosis (Figure 2L) and switched the microglia polarization from pro-inflammatory M1 phenotype to anti-inflammatory M2 phenotype in the hippocampus (Figure 2M). These effects were associated with a decrease in hippocampal neuron apoptosis (Figure 2N) and an improvement in cognitive function (Figures 2O and S2K). Similarly, NCLX overexpression (Figures 2P and S2L) significantly alleviated high-glucose-induced mitochondrial calcium overload (Figures 2Q and S2M) and oxidative damage in *in vitro*-expanded human and mice Treg cells (Figures 2R–2U and S2N–S2Q), followed by M2 microglia polarization and reduced hippocampal neuron death in the coculture systems (Figures 2V and 2W). Collectively, these findings suggest that high-glucose-mediated downregulation of NCLX induces mitochondrial calcium overload and oxidative damage in Treg cells, thereby polarizing microglia toward a pro-inflammatory M1 phenotype and impairing cognitive function in diabetes.

SP1-mediated HDAC2 recruitment and histone deacetylation lead to NCLX downregulation and Treg cell function impairment under high glucose conditions

Based on the aforementioned findings that the mRNA levels of NCLX were decreased in Treg cells under high glucose conditions, it was reasonable to speculate that high glucose might repress NCLX expression through certain transcription factors. We used online tool ALGGEN to identify potential transcription factors that could downregulate NCLX expression. Of all these transcription factors, three (SP1, CEBPB, and YY1) putative transcription factors were identified with R values greater than 0.7 (Figure 3A); more importantly, only SP1 overexpression downregulated NCLX gene expression in high-glucose-treated human and mice Treg cells (Figures 3B and S3A).

We hypothesize that SP1 is a key regulatory factor involved in the suppression of NCLX in Treg cells under high glucose conditions. To test this hypothesis, we first performed chromatin immunoprecipitation (ChIP) in Treg cells isolated from type 2 diabetic patients with MCI as well as nondiabetic controls to determine whether SP1 enrichment occurred in the promoter region of NCLX gene. As shown in Figure 3C, binding of SP1 to the promoter of NCLX was higher in type 2 diabetic patients with MCI than in nondiabetic controls. Similar results were also obtained in *in vitro*-expanded human Treg cells treated with high glucose (Figure S3B). These data highlighted the potential role of SP1 in downregulating NCLX transcription via actions at the NCLX promoter under high glucose conditions. It is well established that SP1 recruits histone deacetylases (HDACs) to inhibit gene expression^{19–21}; we therefore investigated whether SP1 binding to NCLX promoter was associated with changes in histone acetylation that would downregulate NCLX expression. As shown in Figure 3D, we found reduced histone3 (H3) acetylation on the NCLX promoter in Treg cells isolated from type 2 diabetic patients with MCI as compared with nondiabetic controls. Similarly, this change was also observed *in vitro*-expanded human Treg cells treated with high glucose (Figure S3C). To identify responsible HDAC subtype for NCLX downregulation, we examined the physical interaction of SP1 with HDAC1, 2, 4, and 6 through co-immunoprecipitation. Both *in vitro* and *in vivo* experiments demonstrated that SP1 interacted with HDAC1, 2, and 4 in Treg cells. However, only the formation of SP1-HDAC2 complex was significantly increased under high glucose conditions (Figures 3E and S3D); more importantly, the HDAC2 inhibitor, Santacruzamate A (CAY10683), prevented NCLX downregulation in Treg cells under high glucose conditions, suggesting a potential role for the SP1-HDAC2 interaction in downregulating NCLX expression (Figures 3F, 3G, S3E, and S3F). To further confirm that NCLX downregulation in Treg cells under high glucose conditions can be a direct result of SP1-mediated epigenetic regulation, high-glucose-treated human and mice Treg cells were transfected with

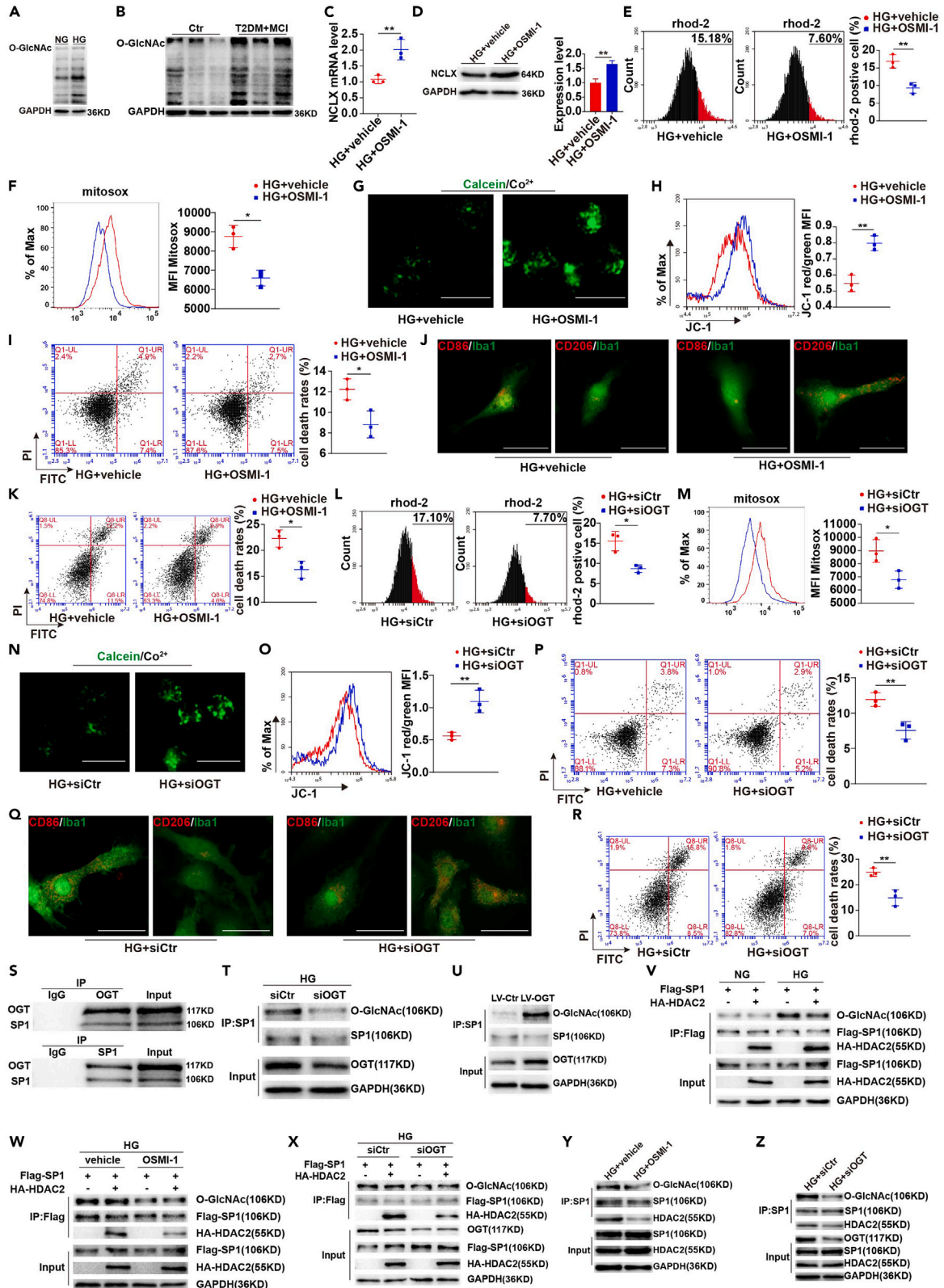


Figure 4. Increasing O-GlcNAcylation of SP1 at S491A contributes to high-glucose-induced effects in Treg cells

- (A) Immunoblots analysis of protein level of O-GlcNAcylation in human Treg cells treated with normal glucose (NG, 5.5 mmol/L D-glucose) or high glucose (HG, 25 mmol/L D-glucose).
- (B) Immunoblot analysis of protein level of O-GlcNAcylation in Treg cells isolated from control subjects and type 2 diabetic patients with MCI.
- (C–I) mRNA level of NCLX (C), quantification analysis of protein level of NCLX (D), flow cytometry analysis of mitochondrial calcium levels (E), mtROS levels (F), MPTP opening (G), MMP (H), and apoptosis levels (I) in human Treg cells treated with or without OGT inhibitors OSMI-1 (30 μ M) in the presence of high glucose (HG, 25 mmol/L D-glucose).
- (J) Representative images for CD86 and CD206 in microglia cocultured with high-glucose (HG, 25 mmol/L D-glucose)-treated Treg cells in the presence or absence of OSMI-1 (30 μ M) for 24 h.
- (K) Flow cytometry analysis of apoptosis in primary hippocampal neurons cocultured with microglia under different treatment. [Samples: (1) HG + vehicle, (2) HG + OSMI-1]. Quantitative data show percentage of cell death rates.
- (L–P) Flow cytometry analysis of mitochondrial calcium levels (L), mtROS levels (M), MPTP opening (N), MMP (O), and apoptosis levels (P) in human Treg cells treated with control siRNA or OGT siRNA in the presence of high glucose (HG, 25 mmol/L D-glucose).
- (Q) Representative images for CD86 and CD206 in microglia cocultured with high-glucose (HG, 25 mmol/L D-glucose)-treated Treg cells in the presence of control siRNA or OGT siRNA.
- (R) Flow cytometry analysis of apoptosis in primary hippocampal neurons cocultured with microglia under different treatment. [Samples: (1) HG + siCtr, (2) HG + siOGT]. Quantitative data show percentage of cell death rates.
- (S) The interaction between OGT and SP1 in human Treg cells was detected by immunoprecipitation and western blot.
- (T) Lysates from human Treg cells treated with high glucose (HG, 25 mmol/L D-glucose) in the presence of control siRNA or OGT siRNA for 72 h were subjected to IP with either control normal IgG or anti-SP1, followed by IB with the indicated antibodies.
- (U) Lysates from human Treg cells infected with OGT-overexpressing lentivirus or control lentivirus for 72 h were subjected to IP with either control normal IgG or anti-SP1, followed by IB with the indicated antibodies.
- (V) HEK293T cells were transfected with Flag-SP1 in the presence or absence of HA-HDAC2 as indicated. After incubation with normal glucose (NG, 5.5 mmol/L D-glucose) or high glucose (HG, 25 mmol/L D-glucose), cells were lysed for precipitated protein detection by Co-immunoprecipitation assay with anti-Flag beads and western blot with indicated antibodies.
- (W) HEK293T cells were transfected with Flag-SP1 in the presence or absence of HA-HDAC2 as indicated. After overnight incubation with or without OSMI-1 (30 μ M) in the presence of high glucose (HG, 25 mmol/L D-glucose), cells were lysed for precipitated protein detection by Co-immunoprecipitation assay with anti-Flag beads and western blot with indicated antibodies.
- (X) HEK293T cells were transfected with Flag-SP1 in the presence or absence of HA-HDAC2 as indicated. After 72 h incubation with control siRNA or OGT siRNA in the presence of high glucose (HG, 25 mmol/L D-glucose), cells were lysed for precipitated protein detection by Co-immunoprecipitation assay with anti-FLAG beads and western blot with indicated antibodies.
- (Y) Lysates from human Treg cells treated with or without OSMI-1 (30 μ M) in the presence of high glucose (HG, 25 mmol/L D-glucose) were subjected to IP with either control normal IgG or anti-SP1, followed by IB with the indicated antibodies.
- (Z) Lysates from human Treg cells treated with high glucose (HG, 25 mmol/L D-glucose) in the presence of control siRNA or OGT siRNA for 72 h were subjected to IP with either control normal IgG or anti-SP1, followed by IB with the indicated antibodies.

a small interfering RNA (siRNA) specific for knockdown of SP1. As expected, SP1 knockdown significantly reversed high-glucose-induced decrease in histone acetylation and the associated increase in SP1 enrichment on NCLX promoter and SP1-HDAC2 complex expression (Figures 3H–3J and S3G–S3I). This was associated with restoration of Treg cell function as evidenced by decreased mitochondrial calcium concentrations (Figures 3K and S3J) and oxidative damage (Figures 3L–3O and S3K–S3N) in Treg cell, increased M2 microglia polarization, and reduced hippocampal neuron apoptosis in the coculture system (Figures 3P and 3Q). Taken together, these results suggest that high glucose increases SP1 enrichment on NCLX promoter in Treg cells, which might cause HDAC2 recruitment and histone deacetylation to repress NCLX expression, and consequently impairs Treg cell function, polarizes microglia toward an M1 phenotype, and promotes neuronal apoptosis.

Increasing O-GlcNAcylation of SP1 at T491 contributes to high-glucose-induced effects in Treg cells

Abnormal O-GlcNAcylation is increasingly recognized as a major pathogenic mechanism of diabetic complications.²² To understand how high glucose induces downregulation of NCLX and mitochondrial oxidative damage in Treg cells, we analyzed the global O-GlcNAcylation levels of *in vitro*-expanded human and mice Treg cells under high glucose treatment. As shown in Figures 4A and S4A, both human and mice Treg cells contained higher levels of global O-GlcNAcylation under high glucose treatment. Similarly, this observation was further confirmed in Treg cells isolated from type 2 diabetic patients with MCI and from db/db mice (Figures 4B and S4B). Cellular O-GlcNAcylation homeostasis is maintained in coordinated fashion by enzymes O-GlcNAc transferase (OGT) and O-GlcNAcase (OGA).^{22,23} To examine whether O-GlcNAcylation of proteins is necessary for high-glucose-induced downregulation of NCLX in Treg cells, we measured the mRNA and protein levels of NCLX in *in vitro*-expanded human and mice Treg cells treated with high glucose in the presence or absence of OGT inhibitor OSMI-1 and found that OGT inhibitor treatment significantly reversed high-glucose-induced downregulation of NCLX in Treg cells (Figures 4C, 4D, S4C, and S4D). Furthermore, this treatment significantly alleviated mitochondrial calcium overload (Figures 4E and S4E) and oxidative damage (Figures 4F–4H and S4F–S4H) in high-glucose-treated Treg cells. These results were accompanied by decreased Treg cell apoptosis (Figures 4I and S4I), enhanced M2 polarization of microglia (Figure 4J), and reduced hippocampal neuron death in the coculture systems (Figure 4K). Similarly, OGT knockdown also subdued high-glucose-induced effects in Treg cells (Figures 4L–4P and S4J–S4N) and in the coculture system (Figures 4Q and 4R). Taken together, these results suggest that elevation of O-GlcNAcylation mediates high-glucose-induced downregulation of NCLX and mitochondrial oxidative damage in Treg cells.

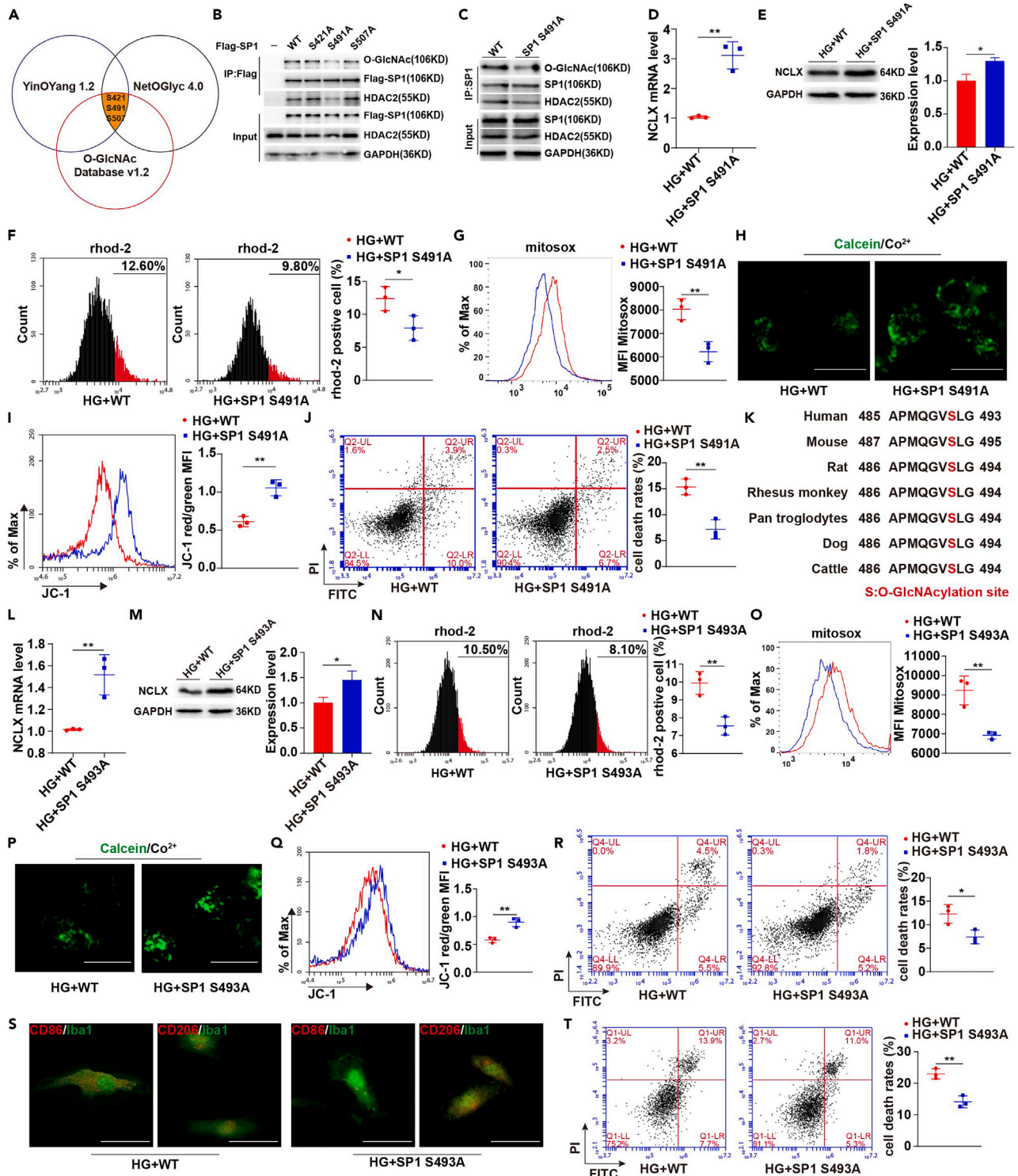


Figure 5. Increasing O-GlcNAcylation of SP1 at S491A contributes to high-glucose-induced effects in Treg cells

(A) O-glycosylation sites were predicted using YinOYang 1.2, NetOGlyc 4.0, and the O-GlcNAc database (v1.2).

(B) Endogenous SP1 was depleted in HEK293T cells by short RNA (shRNA), followed by stable reconstitution with cDNAs encoding WT or O-GlcNAcylation-deficient mutants of SP1 (S421A, S491A, S507A), and SP1 O-GlcNAcylation was analyzed by immunoprecipitation with anti-FLAG antibody and western blot with the indicated antibodies.

Figure 5. Continued

(C) Endogenous SP1 was depleted in high-glucose (HG, 25 mmol/L D-glucose)- treated human Treg cells by short RNA (shRNA), followed by stable reconstitution with cDNAs encoding WT or O-GlcNAcylation-deficient mutants of SP1 (S491A), and SP1 O-GlcNAcylation was analyzed by immunoprecipitation with anti-FLAG antibody and western blot with the indicated antibodies.

(D–J) mRNA level of NCLX (D), quantification analysis of protein level of NCLX (E), flow cytometry analysis of mitochondrial calcium levels (F), mtROS levels (G), MPTP opening (H), MMP (I), and apoptosis levels (J) in human SP1-KD Treg cells under different treatment. [Samples: (1) HG + WT, (2) HG + SP1 S491A].

(K) Cross-species sequence alignment of SP1.

(L–R) mRNA level of NCLX (L), quantification analysis of protein level of NCLX (M), flow cytometry analysis of mitochondrial calcium levels (N), mtROS levels (O), MPTP opening (P), MMP (Q), and apoptosis levels (R) in SP1-KD mouse Treg cells under different treatment. [Samples: (1) HG + WT, (2) HG + SP1 S493A].

(S) Representative images for CD86 and CD206 in microglia cocultured with SP1-KD Treg cells under different treatment. [Samples: (1) HG + WT, (2) HG + SP1 S493A].

(T) Flow cytometry analysis of apoptosis in primary hippocampal neurons cocultured with microglia under different treatment. [Samples: (1) HG + WT, (2) HG + SP1 S493A]. Quantitative data show percentage of cell death rates.

Based on the aforementioned findings that either O-GlcNAcylation inhibition or SP1 knockdown reversed the high-glucose-induced effects in Treg cells, it is likely that downregulation of NCLX expression through SP1 O-GlcNAcylation may be responsible for the observed effects. Reciprocal endogenous immunoprecipitation in human and mice Treg cells confirmed that OGT binds SP1 (Figures 4S and S4O). To further examine whether SP1 was O-GlcNAcyated by OGT, we overexpressed OGT or knocked down OGT, immunoprecipitated SP1, blotted with anti-O-GlcNAc antibody. As shown in Figures 4T, 4U, S4P, and S4Q, knockdown or overexpression of OGT significantly decreased or increased SP1 O-GlcNAcylation in human and mice Treg cells, respectively. Collectively, OGT interacted with O-GlcNAcyated SP1.

Because SP1 increased HDAC2 recruitment on NCLX promoter in Treg cells under high glucose conditions, it is likely that increasing O-GlcNAcylation might promote binding of SP1 and HDAC2. To verify this possibility, we ectopically expressed SP1 alone, or SP1 with HDAC2 in HEK293T cells treated with or without high glucose, and then performed immunoprecipitation. As shown in Figure 4V, high glucose treatment enhanced SP1 O-GlcNAcylation and increased the binding of HDAC2 to SP1. However, OGT inhibitors or OGT knockdown successfully reversed the above effects induced by high glucose (Figures 4W and 4X). Next, we tested whether SP1 O-GlcNAcylation affected the interaction with endogenous HDAC2 in Treg cells. As shown in Figure S4R, the endogenous SP1 was highly glycosylated in human Treg cells treated with high glucose and formed an increased SP1-HDAC2 complex. Similarly, all these high-glucose-induced effects in Treg cells were significantly reversed by OGT inhibitors or OGT knockdown (Figures 4Y and 4Z). Moreover, hyper-O-GlcNAcylation of SP1 and increased binding of HDAC2 to SP1 were also detected in Treg cells isolated from type 2 diabetic patients with MCI and db/db mice (Figures S4S and S4T), suggesting that high-glucose-mediated SP1 O-GlcNAcylation promoted the binding of HDAC2 to SP1 both *in vivo* and *in vitro*.

Performing O-GlcNAcylation prediction analysis in the O-GlcNAc database v1.2 (<https://www.oglcnac.mcw.edu>), we found that S421, S491, and S507 were highly confident O-GlcNAcylation sites on SP1 (Figure 5A). We generated S421A, S491A, and S507A mutants for COIP analysis and identified that only S491A was necessary for both SP1 O-GlcNAcylation and SP1-HDAC2 complex formation in HEK293T cells (Figure 5B). Furthermore, when we ectopically overexpressed SP1 S491A in human Treg cells with endogenous SP1 knockdown (SP1-KD), these cells no longer had high-glucose-induced increase in SP1 O-GlcNAcylation and SP1-HDAC2 complex formation (Figure 5C). Consistent with these results, SP1 S491A mutant significantly reversed high-glucose-induced NCLX downregulation (Figures 5D and 5E) and mitochondrial calcium overload in Treg cells (Figure 5F), accompanied by a decrease in mitochondrial oxidative damage (Figures 5G–5I) and Treg cell apoptosis (Figure 5J). SP1 serine 491 is conserved in human, mice, rat, and other species (Figure 5K). The S491A mutation in human SP1 corresponds to S493A in mouse SP1. Similar results were also observed when SP1 S493A was ectopically overexpressed in SP1-KD mice Treg cells (Figures 5L–5R). Notably, SP1 S493A mutant restored the damaged M2 polarization of microglia and reduced hippocampal neuron death in the coculture systems (Figures 5S and 5T). Taken together, these data suggest that high-glucose-induced NCLX downregulation and Treg cell dysfunction are mediated by SP1 O-GlcNAcylation at its S491A site, which enhances the binding of HDAC2 to SP1 and histone deacetylation on NCLX promoter.

Glucagon-like peptide-1 receptor agonist protects against high glucose-induced Treg cell dysfunction and cognitive impairment through inhibiting SP1 O-GlcNAcylation

Accumulating experimental and clinical evidences demonstrated that GLP-1 receptor agonist improved cognitive impairment in diabetes.^{1,24} Based on the aforementioned findings that Treg cell dysfunction was implicated in the pathogenesis of diabetes-associated cognitive impairment, we examined whether GLP-1 receptor agonist (liraglutide) could alleviate Treg cell dysfunction both *in vivo* and *in vitro*. As shown in Figures 6A–6F, GLP-1 receptor agonist significantly upregulated NCLX expression (Figure 6A) and reduced mitochondrial calcium concentrations (Figure 6B) and oxidative damage (Figures 6C–6F) in Treg cells isolated from db/db mice. These results were accompanied by restoration of M2 microglia polarization (Figure 6G) and improved cognitive function (Figures 6H, 6I, and S5A). Similar effects were also observed in type 2 diabetic patients with MCI (Figures S5B–S5F). To confirm the aforementioned *in vivo* findings, we further tested the effect of GLP-1 receptor agonist on Treg cell function in *in vitro*-expanded human and mice Treg cells. Consistently, high-glucose-induced mitochondrial calcium overload and oxidative damage in human and mice Treg cells could be prevented by GLP-1 receptor agonist (Figures 6J–6N and S5G–S5K). Additionally, GLP-1 receptor agonist protected against high-glucose-induced M1 microglia polarization and hippocampal neuron apoptosis in the coculture system (Figures S5L–S5M).

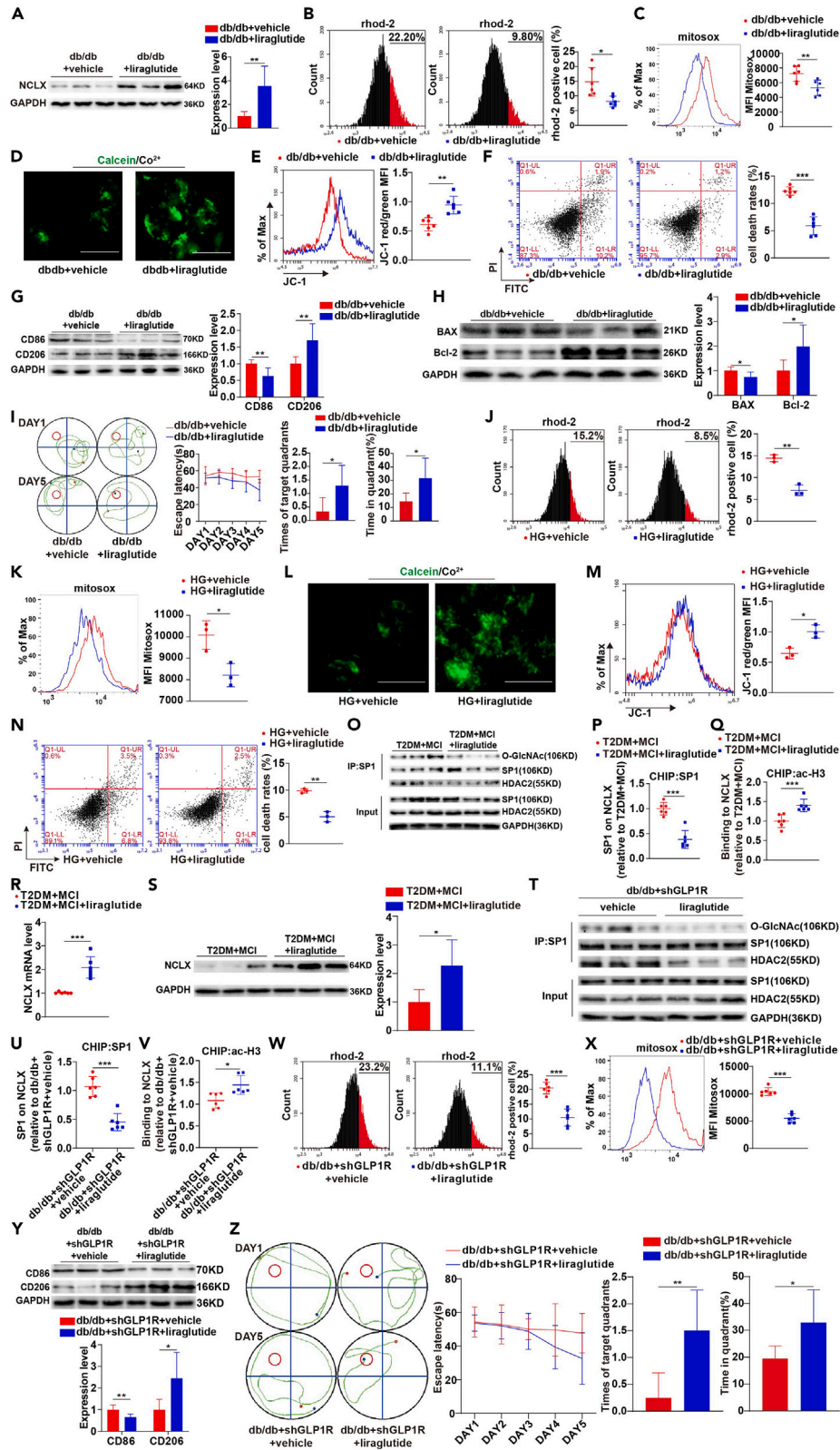


Figure 6. Glucagon-like peptide-1 (GLP-1) receptor agonist protects against high-glucose-induced Treg cell dysfunction and cognitive impairment through inhibiting SP1 O-GlcNAcylation

(A–F) Immunoblots and quantification analysis of protein level of NCLX (A), flow cytometry analysis of mitochondrial calcium levels (B), mtROS levels (C), MPTP opening (D), MMP (E), and apoptosis levels (F) in Treg cells isolated from db/db + vehicle and db/db + liraglutide mice.

(G and H) Immunoblots and quantification analysis of protein levels of CD86, CD206 (G) and BAX, Bcl-2 (H) in the hippocampus of db/db + vehicle and db/db + liraglutide mice.

(I) Morris water maze behavioral assessment for db/db + vehicle or db/db + liraglutide mice showing differences in path (left), escape latency (second from left), number of times mice passed through the platform location in the probe trial (second from right), and the time mice stayed in the target quadrant (right) during learning session.

(J–N) Flow cytometry analysis of mitochondrial calcium levels (J), mtROS levels (K), MPTP opening (L), MMP (M), and apoptosis levels (N) in human Treg cells treated with or without liraglutide (100 nM) in the presence of high glucose (HG, 25 mmol/L D-glucose).

(O) Lysates from Treg cells isolated from type 2 diabetic patients with MCI before and after liraglutide treatment were subjected to IP with either control normal IgG or anti-SP1, followed by IB with the indicated antibodies.

(P) Binding of SP1 to the NCLX promoter in Treg cells isolated from type 2 diabetic patients with MCI before and after liraglutide treatment.

(Q) Levels of histone H3 lysine acetylation (ac-H3) on the NCLX promoter in Treg cells isolated from type 2 diabetic patients with MCI before and after liraglutide treatment.

(R and S) mRNA level of NCLX (R) and quantification analysis of protein level of NCLX (S) in Treg cells isolated from type 2 diabetic patients with MCI before and after liraglutide treatment.

(T) Lysates from Treg cells isolated from db/db + shGLP1R + vehicle and db/db + shGLP1R + liraglutide mice were subjected to IP with either control normal IgG or anti-SP1, followed by IB with the indicated antibodies.

(U) Binding of SP1 to the NCLX promoter in Treg cells isolated from db/db + shGLP1R + vehicle and db/db + shGLP1R + liraglutide mice.

(V) Levels of histone H3 lysine acetylation (ac-H3) on the NCLX promoter in Treg cells isolated from db/db + shGLP1R and db/db + shGLP1R + liraglutide mice.

(W and X) Flow cytometry analysis of mitochondrial calcium levels (W) and mtROS levels (X) in Treg cells isolated from db/db + shGLP1R + vehicle and db/db + shGLP1R + liraglutide mice.

(Y) Immunoblots and quantification analysis of protein levels of CD86 and CD206 in the hippocampus of db/db + shGLP1R + vehicle and db/db + shGLP1R + liraglutide mice.

(Z) Morris water maze behavioral assessment for db/db + shGLP1R + vehicle and db/db + shGLP1R + liraglutide mice showing differences in path (left), escape latency (second from left), number of times mice passed through the platform location in the probe trial (second from right), and the time mice stayed in the target quadrant (right) during learning session.

We next tested whether GLP-1 receptor agonist could reverse the observed effects of high glucose on SP1 O-GlcNAcylation and NCLX expression in Treg cells. As shown in [Figures 6O–6S](#), type 2 diabetic patients with MCI and db/db mice treated with GLP-1 receptor agonist both exhibited reduced SP1 O-GlcNAcylation, decreased HDAC2 recruitment on NCLX promoter, and enhanced NCLX expression in Treg cells. Similar effects were also observed when we treated *in vitro*-expanded human Treg cells with GLP-1 receptor agonist under high glucose conditions ([Figures S5N–S5R](#)).

It is well established that GLP-1 receptor agonist alleviated diabetes-associated cognitive impairment through interacting with GLP-1 receptor in the hippocampus.²⁵ We next examined whether GLP-1-receptor-agonist-mediated improvement in Treg cell function and cognitive performance is independent of GLP-1 receptor signaling in the hippocampus. shRNA was used to knockdown GLP-1R in the hippocampus of db/db mice, and results indicated that GLP-1R knockdown db/db mice treated with GLP-1 receptor agonist still exhibited reduced SP1 O-GlcNAcylation, decreased HDAC2 recruitment on NCLX promoter, and enhanced NCLX expression in Treg cells ([Figures 6T–6V](#), [S5S](#), and [S5T](#)). These results were associated with improved Treg cell function ([Figures 6W](#), [6X](#), [S5U](#), and [S5W](#)), increased M2 microglia polarization ([Figure 6Y](#)), decreased hippocampal neuron apoptosis ([Figure S5X](#)), and better cognitive performance ([Figures 6Z](#) and [S5Y](#)). Collectively, our findings suggest that GLP-1 receptor agonist protects against high-glucose-induced Treg cell dysfunction and cognitive impairment through inhibiting SP1 O-GlcNAcylation and upregulating NCLX expression; importantly, these effects are independent of GLP-1 receptor signaling in the hippocampus.

GLP-1 receptor agonist alleviates high-glucose-induced effects via GLP-1-receptor-mediated upregulation of OGA in Treg cells

The mechanism by which GLP-1 receptor agonist inhibited SP1 O-GlcNAcylation in Treg cells was further investigated. Another factor affecting O-GlcNAc level in cells is the imbalance between OGT and OGA. It has been suggested that OGT and OGA are the only enzymes known to be responsible for adding and removing GlcNAc on serine and threonine residues of target proteins.^{22,23} Interestingly, GLP-1 receptor agonist treatment did not affect OGT but upregulated OGA expression both *in vivo* and *in vitro* ([Figures 7A–7D](#) and [S6A–S6D](#)). To further examine whether GLP-1-receptor-agonist-mediated protection in Treg cells is dependent on OGA upregulation, we transfected high-glucose-treated Treg cells with either scramble (negative control) or OGA siRNA in the presence of GLP-1 receptor agonist. As shown in [Figures 7E–7I](#) and [S6E–S6I](#), GLP-1-receptor-agonist-induced decreases in SP1 O-GlcNAcylation, HDAC2 recruitment, and histone deacetylation on NCLX promoter and increases in NCLX expression under high glucose conditions could be prevented by OGA silencing in human and mice Treg cells. In addition, OGA knockdown further abolished the protective effects of GLP-1 receptor agonist on Treg cell function ([Figures 7J–7N](#) and [S6J–S6M](#)) and M2 microglia polarization ([Figure S6N](#)). Collectively, these findings demonstrate that GLP-1 receptor agonist alleviates high-glucose-induced effects by upregulating OGA expression in Treg cells.

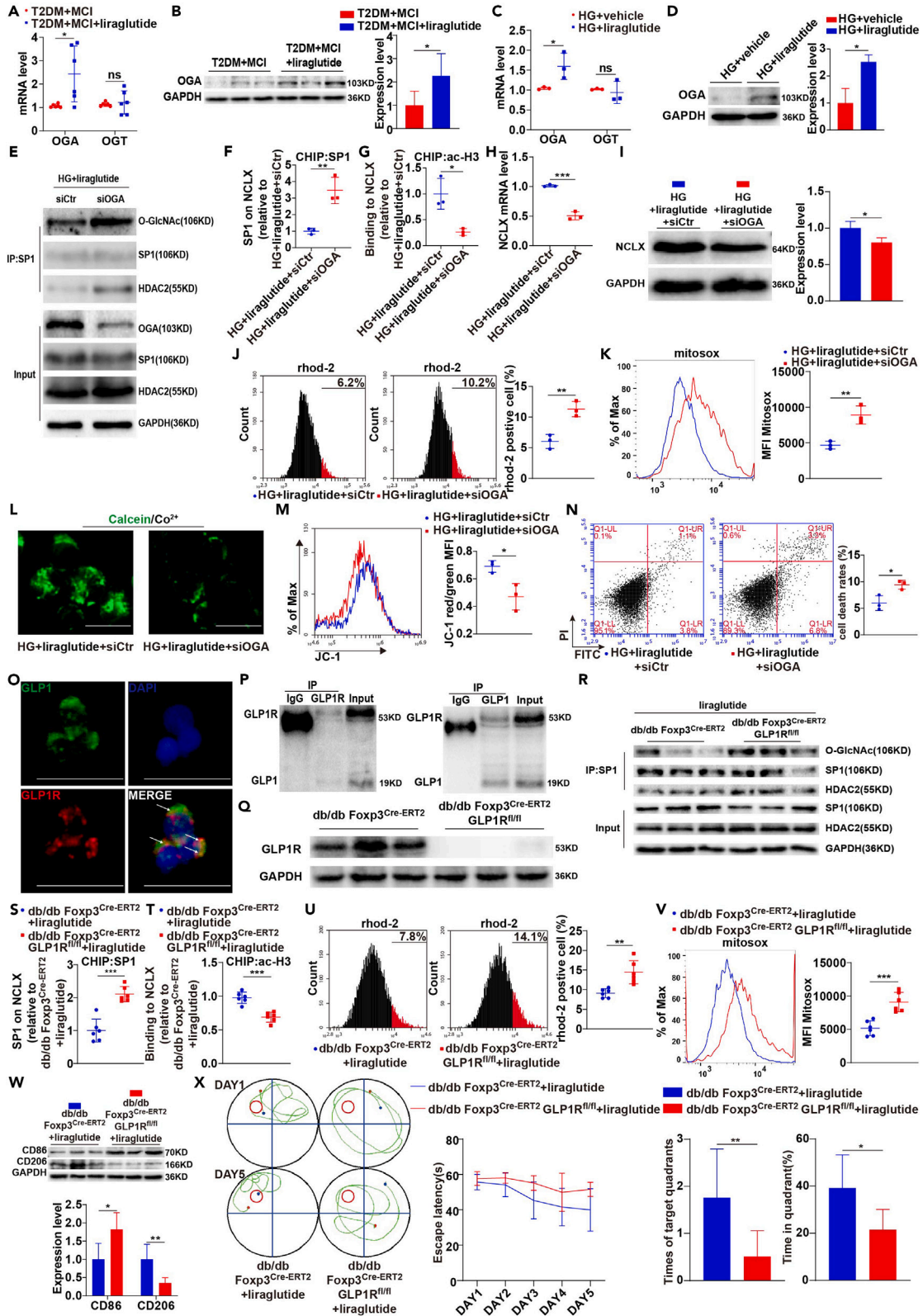


Figure 7. GLP-1 receptor agonist alleviates high-glucose-induced effects via GLP-1-receptor-mediated upregulation of OGA in Treg cells

(A and B) mRNA levels of OGT, OGA (A) and quantification analysis of protein level of OGA (B) in Treg cells isolated from type 2 diabetic patients with MCI before and after liraglutide treatment.

(C and D) mRNA levels of OGT, OGA (C) and quantification analysis of protein level of OGA (D) in human Treg cells treated with or without liraglutide (100 nM) in the presence of high glucose (HG, 25 mmol/L D-glucose).

(E) Lysates from human Treg cells treated with control siRNA or OGA siRNA in the presence of high glucose (HG, 25 mmol/L D-glucose) and liraglutide (100 nM) were subjected to IP with either control normal IgG or anti-SP1, followed by IB with the indicated antibodies.

(F) Binding of SP1 to the NCLX promoter in human Treg cells treated with control siRNA or OGA siRNA in the presence of high glucose (HG, 25 mmol/L D-glucose) and liraglutide (100 nM).

(G) Levels of histone H3 lysine acetylation (ac-H3) on the NCLX promoter in human Treg cells treated with control siRNA or OGA siRNA in the presence of high glucose (HG, 25 mmol/L D-glucose) and liraglutide (100 nM).

(H–N) mRNA levels of NCLX (H), quantification analysis of protein levels of NCLX (I), flow cytometry analysis of mitochondrial calcium levels (J), mtROS levels (K), MPTP opening (L), MMP (M), and apoptosis levels (N) in human Treg cells treated with control siRNA or OGA siRNA in the presence of high glucose (HG, 25 mmol/L D-glucose) and liraglutide (100 nM).

(O) Double immunofluorescence demonstrates co-localization of GLP1 and GLP1R in human Treg cells; arrowheads indicate the co-localization of GLP1 and GLP1R (scale bar, 10 μ m).

(P) The interaction between GLP1 and GLP1R in human Treg cells was detected by immunoprecipitation and western blot.

(Q) Immunoblots analysis of protein level of GLP1R in Treg cells isolated from db/db Foxp3^{Cre-ERT2} and db/db Foxp3^{Cre-ERT2} GLP1R^{fl/fl} mice.

(R) Lysates from Treg cells isolated from db/db Foxp3^{Cre-ERT2} + liraglutide and db/db Foxp3^{Cre-ERT2} GLP1R^{fl/fl} + liraglutide mice were subjected to IP with either control normal IgG or anti-SP1, followed by IB with the indicated antibodies.

(S) Binding of SP1 to the NCLX promoter in Treg cells isolated from db/db Foxp3^{Cre-ERT2} + liraglutide and db/db Foxp3^{Cre-ERT2} GLP1R^{fl/fl} + liraglutide mice.

(T) Levels of histone H3 lysine acetylation (ac-H3) on the NCLX promoter in Treg cells isolated from db/db Foxp3^{Cre-ERT2} + liraglutide and db/db Foxp3^{Cre-ERT2} GLP1R^{fl/fl} + liraglutide mice.

(U–W) Flow cytometry analysis of mitochondrial calcium levels (U), mtROS levels (V), and quantification analysis of protein levels of CD86, CD206 (W) in Treg cells isolated from db/db Foxp3^{Cre-ERT2} + liraglutide and db/db Foxp3^{Cre-ERT2} GLP1R^{fl/fl} + liraglutide mice.

(X) Morris water maze behavioral assessment for db/db Foxp3^{Cre-ERT2} + liraglutide and db/db Foxp3^{Cre-ERT2} GLP1R^{fl/fl} + liraglutide mice showing differences in path (left), escape latency (second from left), number of times mice passed through the platform location in the probe trial (second from right), and the time mice stayed in the target quadrant (right) during learning session.

GLP-1 receptor agonist has been proved to exert pleiotropic effects on cellular signaling and functions via its corresponding receptor. Interestingly, we also found that Treg cells expressed GLP-1 receptor. Therefore, we next tested whether GLP-1 receptor agonist could up-regulate OGA expression via GLP-1 receptor in Treg cells. As shown in Figures 7O and S6O, immunofluorescence staining analysis showed co-localization of GLP-1 and GLP-1 receptor on the surface of human and mice Treg cells. Meanwhile, COIP assays demonstrated that GLP-1 could be pulled down by using GLP-1 receptor as the precipitating antibody in human and mice Treg cells and vice versa (Figures 7P and S6P). To directly examine whether GLP-1/GLP-1 receptor signaling protect against high-glucose-induced effects *in vivo*, we generated db/db mice with Treg-cell-specific deletion of GLP-1 receptor by using tamoxifen-inducible Cre recombinase driven by endogenous Foxp3 locus to delete the loxP-flanked GLP-1 receptor gene after FOXP3 was expressed in Treg cells (Figure 7Q). GLP-1-receptor-agonist-induced decreases in SP1 O-GlcNAcylation, HDAC2 recruitment, and histone deacetylation on NCLX promoter and increases in OGA and NCLX expression were significantly abolished in Foxp3^{Cre-ERT2} GLP-1R^{fl/fl} db/db mice after tamoxifen treatment (Figures 7R–7T and S6Q, and S6R). Consistently, GLP-1 receptor knockout in Treg cells significantly abolished the protective effects of GLP-1 receptor agonist on Treg cell function (Figures 7U, 7V, and S6S–S6U), M2 microglia polarization (Figure 7W), hippocampal neuron apoptosis (Figure S6V), and cognitive performance in db/db mice (Figures 7X and S6W). Similar effects were also observed when we transfected *in vitro*-expanded human and mice Treg cells with siRNA targeting GLP-1 receptor (Figures S7A–S7V). Together, these findings reveal that GLP-1 receptor agonist protects against high-glucose-induced effects via GLP-1-receptor-mediated upregulation of OGA in Treg Cells.

DISCUSSION

In the present study, we elucidate a mechanism underlying high-glucose-induced Treg cell dysfunction and cognitive impairment in type 2 diabetes. The key findings of this work are summarized as follows: (1) high glucose impairs Treg cell function through mitochondrial calcium overload and induces M1 microglia polarization and cognitive impairment in type 2 diabetes. (2) High glucose O-GlcNAcylation transcriptional factor SP1 at Ser491, leading to enhanced HDAC2 recruitment and histone deacetylation on NCLX promoter, which downregulates NCLX expression and induces mitochondrial calcium overload and oxidative damage in Treg cells. (3) GLP-1 receptor agonist alleviates these deleterious effects in type 2 diabetes via GLP-1-receptor-mediated upregulation of OGA and inhibition of SP1 O-GlcNAcylation in Treg cells.

Hyperglycemia is associated with an increased risk of cognitive impairment in elderly type 2 diabetic patients.²⁶ It was also noted that the peripheral frequencies of CD4⁺CD25⁺Foxp3⁺ Treg cells were significantly lower in type 2 diabetic patients compared with nondiabetic controls.²⁷ Intriguingly, there are few studies investigating the effects of high glucose on Treg cell function and its association with cognitive performance in type 2 diabetes. In this study, we found that Treg cells exhibited increased mtROS production, MPTP opening, and apoptosis under high glucose conditions, and these effects were accompanied by a decrease in MMP, mtDNA content, and ATP generation, indicating that high glucose exerted detrimental effects on Treg cells by promoting mitochondrial dysfunction and inducing oxidative damage. In addition, scavenging of mtROS in Treg cells alleviated these deleterious effects in type 2 diabetes, which was consistent with previous study demonstrating that therapeutic mtROS scavenging significantly improved Treg cell dysfunction in autoimmunity.⁸ Furthermore, our data indicated that impaired Treg cell

function polarized microglia toward a pro-inflammatory M1 phenotype and promoted neuronal injury and cognitive impairment in type 2 diabetes. This observation implicates that disruption of Treg-microglia crosstalk is involved in diabetes-associated cognitive impairment.

It is reported that impaired mitochondrial calcium homeostasis under diverse pathological conditions initiates calcium overload, resulting in mitochondrial dysfunction and oxidative damage.^{28,29} NCLX is a critical regulator playing an important role in mitochondrial calcium extrusion.¹¹ Interestingly, our results demonstrated that NCLX was downregulated in type 2 diabetes, leading to inhibition of calcium efflux and mitochondrial calcium overload that is critical for inducing oxidative damage to impair Treg cell function. Moreover, both our *in vivo* and *in vitro* data demonstrated that NCLX overexpression successfully alleviated high-glucose-induced mitochondrial calcium overload and oxidative damage in Treg cells, accompanied by an improvement in microglia polarization and cognitive performance. These findings highlight the crucial role of NCLX in maintaining mitochondrial calcium homeostasis and preserving Treg cell function under high glucose conditions, which may facilitate the design of therapies for diabetes-associated cognitive impairment.

O-GlcNAcylation is a posttranslational, bidirectional, dynamic modification of serine and threonine residues linked to glucose metabolism and centrally involved in regulating cellular homeostasis.^{22,23} Abnormal O-GlcNAcylation is increasingly recognized as a general mechanism underlying diabetic complications.²² In this study, we found that high glucose downregulated NCLX expression by increasing SP1 O-GlcNAcylation and enhancing HDAC2 recruitment and histone deacetylation on NCLX promoter, indicating that high-glucose-induced SP1 O-GlcNAcylation is the key factor to impair Treg cell function and cognitive performance in type 2 diabetes. SP1 is a ubiquitous zinc finger transcription factor that positively or negatively regulates gene expression by binding to guanine-cytosine-rich elements in the promoter region of target genes.^{30–32} Interestingly, our data revealed that NCLX expression was downregulated by SP1 in Treg cells under high glucose conditions. Previous studies have shown that SP1 affected downstream gene expression by regulating HDAC2.^{33,34} This was consistent with our finding. However, other studies have revealed that HDAC2 was the upstream of SP1.^{21,35} Therefore, we conjectured that the regulatory relationship between SP1 and HDAC2 was bidirectional. Our results extended those findings and demonstrated that O-GlcNAcylation of SP1 at S491 increased the binding of HDAC2 to SP1 on NCLX promoter, resulting in increased histone deacetylation and downregulation of NCLX expression in Treg cells. Accordingly, Treg-cell-specific SP1 S491A mutation significantly alleviated high-glucose-induced deleterious effects. This modulation of SP1 function through O-GlcNAcylation of SP1 at S491 links glucose and mitochondrial calcium overload in Treg cell, implicating SP1 as a potential therapeutic target for the treatment of Treg cell dysfunction and cognitive impairment in type 2 diabetes.

GLP-1 receptor agonist, a widely used antidiabetic drug, has been proved to exert protective effects on cognitive function in type 2 diabetes.^{1,24,36} The mechanism underlying this phenomenon is largely attributed to activation of GLP-1/GLP-1 receptor signaling in the brain.³⁷ In this study, we also observed an improved cognitive performance in type 2 diabetic patients and db/db mice after GLP-1 receptor agonist treatment. More importantly, GLP-1 receptor agonist still protected db/db mice against high-glucose-induced cognitive impairment after hippocampal knockdown of GLP-1 receptor, suggesting that mechanisms other than activation of GLP-1/GLP-1 receptor signaling in the hippocampus are involved in GLP-1-receptor-agonist-mediated protective effects on cognitive function. Interestingly, we found that GLP-1 receptor was also expressed on the surface of Treg cell. Moreover, GLP-1 receptor agonist upregulated OGA expression in Treg cells via GLP-1 receptor, resulting in a decrease in SP1 O-GlcNAcylation at S491 and subsequently leading to upregulation of NCLX. These effects were accompanied by meaningful improvement in mitochondrial calcium overload, Treg cell dysfunction, and cognitive impairment. Accordingly, Treg-specific deletion of GLP-1 receptor significantly reduced these GLP-1-receptor-agonist-mediated protective effects under high glucose conditions, confirming that regulation of GLP-1 receptor/OGA signaling in Treg cells might serve as another important mechanism for GLP-1-receptor-agonist-mediated neuroprotection in type 2 diabetes.

In conclusion, we report a link between high-glucose-mediated SP1 O-GlcNAcylation and HDAC2/NCLX signaling in control of mitochondrial calcium concentrations in Treg cells. Our study also reveals a mechanism for linking Treg cell dysfunction and cognitive impairment in type 2 diabetes and provides an insight into the mechanism underlying the neuroprotective effects of GLP-1 receptor agonist.

Limitations of the study

The lack of autopsy data is the first limitation of this study, as postmortem analysis would be helpful to further elucidate the crosstalk between Treg and microglia in the brains of type 2 diabetic patients. Furthermore, the upstream mechanisms by which GLP-1 receptor agonist upregulated OGA expression warrants further investigation. Finally, the *in vivo* effects of SP1 S491A mutation on Treg dysfunction and cognitive impairment in diabetes remain uninvestigated.

STAR★METHODS

Detailed methods are provided in the online version of this paper and include the following:

- [KEY RESOURCES TABLE](#)
- [RESOURCE AVAILABILITY](#)
 - Lead contact
 - Materials availability
 - Data and code availability
- [EXPERIMENTAL MODEL AND SUBJECT DETAILS](#)
 - Mice
 - Human samples

- Cell isolation and culture
- **METHOD DETAILS**
 - Gene silencing and overexpression
 - Immunoblot and Co-immunoprecipitation analysis
 - Chromatin immunoprecipitation
 - RNA preparation and quantitative PCR
 - Immunofluorescence
 - ATP measurement
 - Detection of reactive oxygen species (ROS)
 - Apoptosis assays
 - Mitochondrial Ca²⁺ Measurement
 - MPTP
 - Mitochondrial membrane potential measurement
 - Transmission electron microscopy (TEM)
 - Morris water maze
 - Active avoidance memory test
 - Bioinformatics analysis
- **QUANTIFICATION AND STATISTICAL ANALYSIS**

SUPPLEMENTAL INFORMATION

Supplemental information can be found online at <https://doi.org/10.1016/j.isci.2023.108689>.

ACKNOWLEDGMENTS

This study was supported by grants from the National Natural Science Foundation of China (Grant No. 82260171), the Natural Science Foundation of Guangxi Province for Distinguished Young Scholars (Grant No. 2021GXNSFFA196003), the Scientific Research and Technology Development Projects of Science and Technology Department of Guangxi Province (Grant No. 1598012-13), the Natural Science Foundation of Guangxi Province (Grant No. 2015GXNSFBA139119), the Innovation Project of Guangxi Graduate Education (Grant No. YCSW2022378, YCSW2023409, YCSW2023410, YCSW2023424), and the Graduate Research Program of Guilin Medical University (Grant No. GYYK2022016).

AUTHOR CONTRIBUTIONS

T.P.Z. supervised the study and designed the experiments. Y.H., Y.M.Z., and L.Y.K. performed experiments, analyzed results, and generated figures. Y.Y.T. and Z.Q.X. performed data collection. Y.H. and T.P.Z. wrote the manuscript. T.P.Z. reviewed the manuscript.

DECLARATION OF INTERESTS

The authors declare no competing interests.

INCLUSION AND DIVERSITY

We support inclusive, diverse, and equitable conduct of research.

Received: July 4, 2023

Revised: November 2, 2023

Accepted: December 5, 2023

Published: December 13, 2023

REFERENCES

1. Cukierman-Yaffe, T., Gerstein, H.C., Colhoun, H.M., Diaz, R., Garcia-Pérez, L.E., Lakshmanan, M., Bethel, A., Xavier, D., Probstfield, J., Riddle, M.C., et al. (2020). Effect of dulaglutide on cognitive impairment in type 2 diabetes: an exploratory analysis of the REWIND trial. *Lancet Neurol.* *19*, 582–590.
2. Shi, L., Sun, Z., Su, W., Xu, F., Xie, D., Zhang, Q., Dai, X., Iyer, K., Hitchens, T.K., Foley, L.M., et al. (2021). Treg cell-derived osteopontin promotes microglia-mediated white matter repair after ischemic stroke. *Immunity* *54*, 1527–1542.e8.
3. Machhi, J., Kevadiya, B.D., Muhammad, I.K., Herskovitz, J., Olson, K.E., Mosley, R.L., and Gendelman, H.E. (2020). Harnessing regulatory T cell neuroprotective activities for treatment of neurodegenerative disorders. *Mol. Neurodegener.* *15*, 32.
4. Hui, Y., Xu, Z., Li, J., Kuang, L., Zhong, Y., Tang, Y., Wei, J., Zhou, H., and Zheng, T. (2023). Nonenzymatic function of DPP4 promotes diabetes-associated cognitive dysfunction through IGF-2R/PKA/SP1/ERp29/IP3R2 pathway-mediated impairment of Treg function and M1 microglia polarization. *Metabolism* *138*, 155340.
5. Watson, M.J., Vignali, P.D.A., Mullett, S.J., Overacre-Delgoffe, A.E., Peralta, R.M., Grebinoski, S., Menk, A.V., Rittenhouse, N.L., DePeaux, K., Whetstone, R.D., et al. (2021). Metabolic support of tumour-infiltrating regulatory T cells by lactic acid. *Nature* *591*, 645–651.
6. Villa, M., O'Sullivan, D., and Pearce, E.L. (2021). Glucose makes Treg lose their temper. *Cancer Cell* *39*, 460–462.

7. Chen, M., Chen, Z., Wang, Y., Tan, Z., Zhu, C., Li, Y., Han, Z., Chen, L., Gao, R., Liu, L., and Chen, Q. (2016). Mitophagy receptor FUNDC1 regulates mitochondrial dynamics and mitophagy. *Autophagy* 12, 689–702.
8. Alissafi, T., Kalafati, L., Lazari, M., Filia, A., Kloukina, I., Manifava, M., Lim, J.H., Alexaki, V.I., Ktistakis, N.T., Doskas, T., et al. (2020). Mitochondrial Oxidative Damage Underlies Regulatory T Cell Defects in Autoimmunity. *Cell Metabol.* 32, 591–604.e7.
9. Ding, L., Yang, X., Tian, H., Liang, J., Zhang, F., Wang, G., Wang, Y., Ding, M., Shui, G., and Huang, X. (2018). Seipin regulates lipid homeostasis by ensuring calcium-dependent mitochondrial metabolism. *EMBO J.* 37, e97572.
10. Solesio, M.E., Garcia Del Molino, L.C., Elustondo, P.A., Diao, C., Chang, J.C., and Pavlov, E.V. (2020). Inorganic polyphosphate is required for sustained free mitochondrial calcium elevation, following calcium uptake. *Cell Calcium* 86, 102127.
11. Pathak, T., and Trebak, M. (2018). Mitochondrial Ca(2+) signaling. *Pharmacol. Ther.* 192, 112–123.
12. Nita, I.I., Hershinkel, M., Fishman, D., Ozeri, E., Rutter, G.A., Sensi, S.L., Khananashvili, D., Lewis, E.C., and Sekler, I. (2012). The mitochondrial Na⁺/Ca²⁺ exchanger upregulates glucose dependent Ca²⁺ signalling linked to insulin secretion. *PLoS One* 7, e46649.
13. Garbincius, J.F., and Elrod, J.W. (2022). Mitochondrial calcium exchange in physiology and disease. *Physiol. Rev.* 102, 893–992.
14. Schmidleithner, L., Thabet, Y., Schönfeld, E., Köhne, M., Sommer, D., Abdullah, Z., Sadlon, T., Osei-Sarpong, C., Subbaramaiah, K., Copperi, F., et al. (2019). Enzymatic Activity of HPGD in Treg Cells Suppresses Tconv Cells to Maintain Adipose Tissue Homeostasis and Prevent Metabolic Dysfunction. *Immunity* 50, 1232–1248.e14.
15. Kaufmann, U., Kahlfuss, S., Yang, J., Ivanova, E., Koralov, S.B., and Feske, S. (2019). Calcium Signaling Controls Pathogenic Th17 Cell-Mediated Inflammation by Regulating Mitochondrial Function. *Cell Metabol.* 29, 1104–1118.e6.
16. Dia, M., Gomez, L., Thibault, H., Tessier, N., Leon, C., Chouabe, C., Ducreux, S., Gallo-Bona, N., Tubbs, E., Bendridi, N., et al. (2020). Reduced reticulum-mitochondria Ca(2+) transfer is an early and reversible trigger of mitochondrial dysfunctions in diabetic cardiomyopathy. *Basic Res. Cardiol.* 115, 74.
17. Bartok, A., Weaver, D., Golenár, T., Nichtova, Z., Katona, M., Bánsági, S., Alzayady, K.J., Thomas, V.K., Ando, H., Mikoshiba, K., et al. (2019). IP3 receptor isoforms differently regulate ER-mitochondrial contacts and local calcium transfer. *Nat. Commun.* 10, 3726.
18. Jadiya, P., Kolmetzky, D.W., Tomar, D., Di Meco, A., Lombardi, A.A., Lambert, J.P., Luongo, T.S., Ludtmann, M.H., Praticò, D., and Elrod, J.W. (2019). Impaired mitochondrial calcium efflux contributes to disease progression in models of Alzheimer's disease. *Nat. Commun.* 10, 3885.
19. Liu, S., Wu, L.C., Pang, J., Santhanam, R., Schwind, S., Wu, Y.Z., Hickey, C.J., Yu, J., Becker, H., Maharry, K., et al. (2010). Sp1/NFκB/HDAC/miR-29b regulatory network in KIT-driven myeloid leukemia. *Cancer Cell* 17, 333–347.
20. Yuan, J.H., Yang, F., Chen, B.F., Lu, Z., Huo, X.S., Zhou, W.P., Wang, F., and Sun, S.H. (2011). The histone deacetylase 4/SP1/microrna-200a regulatory network contributes to aberrant histone acetylation in hepatocellular carcinoma. *Hepatology* 54, 2025–2035.
21. Zheng, Z., Zhang, S., Chen, J., Zou, M., Yang, Y., Lu, W., Ren, S., Wang, X., Dong, W., Zhang, Z., et al. (2022). The HDAC2/SP1/miR-205 feedback loop contributes to tubular epithelial cell extracellular matrix production in diabetic kidney disease. *Clin. Sci.* 136, 223–238.
22. Chatham, J.C., Zhang, J., and Wende, A.R. (2021). Role of O-Linked N-Acetylglucosamine Protein Modification in Cellular (Patho)Physiology. *Physiol. Rev.* 101, 427–493.
23. Gorelik, A., Bartual, S.G., Borodkin, V.S., Varghese, J., Ferenbach, A.T., and van Aalten, D.M.F. (2019). Genetic recoding to dissect the roles of site-specific protein O-GlcNAcylation. *Nat. Struct. Mol. Biol.* 26, 1071–1077.
24. Rawlings, A.M., Sharrett, A.R., Albert, M.S., Coresh, J., Windham, B.G., Power, M.C., Knopman, D.S., Walker, K., Burgard, S., Mosley, T.H., et al. (2019). The Association of Late-Life Diabetes Status and Hyperglycemia With Incident Mild Cognitive Impairment and Dementia: The ARIC Study. *Diabetes Care* 42, 1248–1254.
25. Park, K.A., Jin, Z., Lee, J.Y., An, H.S., Choi, E.B., Kim, K.E., Shin, H.J., Jeong, E.A., Min, K.A., Shin, M.C., and Roh, G.S. (2020). Long-Lasting Exendin-4 Fusion Protein Improves Memory Deficits in High-Fat Diet/Streptozotocin-Induced Diabetic Mice. *Pharmaceutics* 12, 159.
26. Kim, W.J., Lee, S.J., Lee, E., Lee, E.Y., and Han, K. (2022). Risk of Incident Dementia According to Glycemic Status and Comorbidities of Hyperglycemia: A Nationwide Population-Based Cohort Study. *Diabetes Care* 45, 134–141.
27. SantaCruz-Calvo, S., Bharath, L., Pugh, G., SantaCruz-Calvo, L., Lenin, R.R., Lutshumba, J., Liu, R., Bachstetter, A.D., Zhu, B., and Nikolajczyk, B.S. (2022). Adaptive immune cells shape obesity-associated type 2 diabetes mellitus and less prominent comorbidities. *Nat. Rev. Endocrinol.* 18, 23–42.
28. Murphy, E., and Liu, J.C. (2022). Mitochondrial calcium and reactive oxygen species in cardiovascular disease. *Cardiovasc. Res.* 119, 1105–1116.
29. Tsai, C.W., Rodriguez, M.X., Van Keuren, A.M., Phillips, C.B., Shushunov, H.M., Lee, J.E., Garcia, A.M., Ambardekar, A.V., Cleveland, J.C., Jr., Reisz, J.A., et al. (2022). Mechanisms and significance of tissue-specific MICU regulation of the mitochondrial calcium uniporter complex. *Mol. Cell* 82, 3661–3676.e8.
30. Li, H., Zhang, Y., Ströse, A., Tedesco, D., Gurova, K., and Selivanova, G. (2014). Integrated high-throughput analysis identifies Sp1 as a crucial determinant of p53-mediated apoptosis. *Cell Death Differ.* 21, 1493–1502.
31. Kaczynski, J., Cook, T., and Urrutia, R. (2003). Sp1- and Kruppel-like transcription factors. *Genome Biol.* 4, 206.
32. Liu, H.T., Zou, Y.X., Zhu, W.J., Sen, L., Zhang, G.H., Ma, R.R., Guo, X.Y., and Gao, P. (2022). lncRNA THAP7-AS1, transcriptionally activated by SP1 and post-transcriptionally stabilized by METTL3-mediated m6A modification, exerts oncogenic properties by improving CUL4B entry into the nucleus. *Cell Death Differ.* 29, 627–641.
33. Miao, J., Chen, Z., Wu, Y., Hu, Q., and Ji, T. (2022). Sp1 Inhibits PGC-1α via HDAC2-Catalyzed Histone Deacetylation in Chronic Constriction Injury-Induced Neuropathic Pain. *ACS Chem. Neurosci.* 13, 3438–3452.
34. Zhu, W., Li, Z., Xiong, L., Yu, X., Chen, X., and Lin, Q. (2017). FKBP3 Promotes Proliferation of Non-Small Cell Lung Cancer Cells through Regulating Sp1/HDAC2/p27. *Theranostics* 7, 3078–3089.
35. Xie, L., Zhou, Q., Chen, X., Du, X., Liu, Z., Fei, B., Hou, J., Dai, Y., and She, W. (2021). Elucidation of the Hdac2/Sp1/miR-204-5p/Bcl-2 axis as a modulator of cochlear apoptosis via *in vivo/in vitro* models of acute hearing loss. *Mol. Ther. Nucleic Acids* 23, 1093–1109.
36. Batista, A.F., Forny-Germano, L., Clarke, J.R., Lyra E Silva, N.M., Brito-Moreira, J., Boehnke, S.E., Winterborn, A., Coe, B.C., Lablans, A., Vital, J.F., et al. (2018). The diabetes drug liraglutide reverses cognitive impairment in mice and attenuates insulin receptor and synaptic pathology in a non-human primate model of Alzheimer's disease. *J. Pathol.* 245, 85–100.
37. During, M.J., Cao, L., Zuzga, D.S., Francis, J.S., Fitzsimons, H.L., Jiao, X., Bland, R.J., Klugmann, M., Banks, W.A., Drucker, D.J., and Haile, C.N. (2003). Glucagon-like peptide-1 receptor is involved in learning and neuroprotection. *Nat. Med.* 9, 1173–1179.
38. Bader, M., Li, Y., Tweedie, D., Shlobin, N.A., Bernstein, A., Rubovitch, V., Tovar-Y-Romo, L.B., DiMarchi, R.D., Hoffer, B.J., Greig, N.H., and Pick, C.G. (2019). Neuroprotective Effects and Treatment Potential of Incretin Mimetics in a Murine Model of Mild Traumatic Brain Injury. *Front. Cell Dev. Biol.* 7, 356.
39. Sun, C., Xiao, Y., Li, J., Ge, B., Chen, X., Liu, H., and Zheng, T. (2022). Nonenzymatic function of DPP4 in diabetes-associated mitochondrial dysfunction and cognitive impairment. *Alzheimers Dement.* 18, 966–987.

STAR★METHODS

KEY RESOURCES TABLE

| REAGENT or RESOURCE | SOURCE | IDENTIFIER |
|--|---------------------------|------------------------------------|
| Antibodies | | |
| Anti-GLP-1R | Proteintech | Cat# 26196-1-AP; RRID: AB_2880421 |
| Anti-GLP1R | Santa Cruz Biotechnology | Cat# sc-390774; RRID: AB_2819000 |
| Anti-GLP-1 | Santa Cruz Biotechnology | Cat# sc-73508; RRID: AB_1123550 |
| Anti-SP1 | Cell Signaling Technology | Cat# 9389; RRID: AB_11220235 |
| Anti-SP1 | Santa Cruz Biotechnology | Cat# sc-17824; RRID: AB_628272 |
| Anti-OGT | Proteintech | Cat# 11576-2-AP; RRID: AB_2156943 |
| Anti-O-GlcNAc (CTD110.6) | Cell Signaling Technology | Cat# 98755; RRID: AB_10950973 |
| Anti-OGA | Proteintech | Cat# 14711-1-AP; RRID: AB_2143063 |
| Anti-GAPDH | Proteintech | Cat# 10494-1-AP; RRID: AB_2263076 |
| Anti-NCLX | Proteintech | Cat# 21430-1-AP; RRID: AB_10858637 |
| Anti-HDAC1 | Proteintech | Cat# 10197-1-AP; RRID:AB_2118062 |
| Anti-HDAC2 | Proteintech | Cat# 12922-3-AP; RRID:AB_2118516 |
| Anti-HDAC4 | Proteintech | Cat# 17449-1-AP; RRID:AB_2118864 |
| Anti-HDAC4 | ABCAM | Cat# ab12172; RRID:AB_298904 |
| Anti-HDAC6 | Sigma-Aldrich | Cat# H2287; RRID:AB_477052 |
| Anti-acetyl-Histone H3 | Millipore | Cat# 06-599; RRID:AB_2115283 |
| Anti-Histone H4 | ABCAM | Cat# ab177790; RRID:AB_2732882 |
| Anti-Iba1 | Affinity Biosciences | Cat# DF6442; RRID: AB_2838405 |
| Anti-Iba1 | Santa Cruz Biotechnology | Cat# sc-32725; RRID: AB_667733 |
| Anti-Foxp3 | Santa Cruz Biotechnology | Cat# sc-166212; RRID: AB_2104928 |
| Anti-Foxp3 | Cell Signaling Technology | Cat# 12632S; RRID: AB_2797974 |
| Anti-Foxp3 | BD Biosciences | Cat# 560045; RRID: AB_1645411 |
| Anti-Foxp3 | Thermo Fisher Scientific | Cat# 17-4776-42; RRID: AB_1603280 |
| Anti-CD25 | Thermo Fisher Scientific | Cat# 12-0259-42; RRID: AB_1659682 |
| Anti-CD25 | BD Biosciences | Cat# 555432; RRID: AB_395826 |
| Anti-CD4 | Thermo Fisher Scientific | Cat# 11-0049-42; RRID: AB_1659694 |
| Anti-CD4 | BD Biosciences | Cat# 550628; RRID: AB_393789 |
| Anti-CD206 | Santa Cruz Biotechnology | Cat# sc-58986; RRID: AB_2144945 |
| Anti-CD206 | Proteintech | Cat# 18704-1-AP; RRID: AB_10597232 |
| Anti-CD86 | Santa Cruz Biotechnology | Cat# sc-19617; RRID: AB_627201 |
| Anti-CD86 | Proteintech | Cat# 13395-1-AP; RRID: AB_2074882 |
| Goat anti-mouse IgG | Proteintech | Cat# SA00001-1; RRID: AB_2722565 |
| Goat anti-rabbit IgG | Proteintech | Cat# SA00001-2; RRID: AB_2722564 |
| CoraLite488 – conjugated Affinipure Goat Anti- mouse | Proteintech | Cat# SA00013-1; RRID: AB_2810983 |
| CoraLite488 – conjugated Affinipure Goat Anti-Rabbit | Proteintech | Cat# SA00013-2; RRID: AB_2797132 |
| CoraLite594 – conjugated Affinipure Goat Anti- mouse | Proteintech | Cat# SA00013-3; RRID: AB_2797133 |
| CoraLite594 – conjugated Affinipure Goat Anti-Rabbit | Proteintech | Cat# SA00013-4; RRID: AB_2810984 |
| Chemicals, peptides, and recombinant proteins | | |
| B-27 (50x) | Thermo Fisher Scientific | Cat# 17504044 |
| TRLZOI™ Reagent | invitrogen | Cat# 15596026 |

(Continued on next page)

Continued

| REAGENT or RESOURCE | SOURCE | IDENTIFIER |
|---|--|------------------|
| MonAmp™ SYBR Green qPCR Mix | Monad | Cat# MQ10301S |
| Fastking RT Kit (with gDNA) | TIANGEN | Cat# KR116-02 |
| Poly-L-lysine | Sigma-Aldrich | Cat# P4707 |
| Neurobasal medium | Invitrogen | Cat# 21103049 |
| DMEM | Thermo Fisher Scientific | Cat# 11995065 |
| RPMI 1640 medium, HEPES | Thermo Fisher Scientific | Cat# 22400105 |
| Sodium pyruvate | Thermo Fisher Scientific | Cat# 11360070 |
| TexMACS™ Medium | Miltenyi Biotec | Cat# 130-097-196 |
| Trypsin Digestion solutions,0.25% (without phenol red) | Solarbio | Cat# T1350 |
| DNase I | Roche | Cat# 11284932001 |
| Penicillin-Streptomycin Liquid | Solarbio | Cat# P1400 |
| SPI Chem SPI-Pon™ 812 Kit | SPI-CHEM™ | Cat# GS02660 |
| 2.5% Glutaraldehyde | Solarbio | Cat# P1126 |
| Osmium tetroxide | Beijing Zhongjingkeyi Technology Co., Ltd | Cat# GP18456 |
| Uranyl acetate | Beijing Zhongjingkeyi Technology Co., Ltd | Cat# GZ02625 |
| Lead citrate | Beijing Zhongjingkeyi Technology Co., Ltd | Cat# GZ02618 |
| 4% Paraformaldehyde | Solarbio | Cat# P1110 |
| Quick Antigen Retrieval Solution for Frozen Sections | beyotime | Cat# P0090 |
| QuickBlock™ Primary Antibody Dilution Buffer for Immunol Staining | beyotime | Cat# P0262 |
| QuickBlock™ Secondary Antibody Dilution Buffer for Immunofluorescence | beyotime | Cat# P0265 |
| QuickBlock™ Blocking Buffer for Immunol Staining | beyotime | Cat# P0260 |
| DAPI solution | Solarbio | Cat# C0060 |
| QuickBlock™ Blocking Buffer for Western Blot | beyotime | Cat# P0252 |
| QuickBlock™ Secondary Antibody Dilution Buffer for Western Blot | beyotime | Cat# P0258 |
| QuickBlock™ Primary Antibody Dilution Buffer for Western Blot | beyotime | Cat# P0256 |
| ECL reagent | Shanghai Life-iLab Bio Technolity Co., Ltd | Cat# AP34L024 |
| MitoSOX™ Red mitochondrial superoxide indicator | Thermo Fisher Scientific | Cat# M36008 |
| Rhod-2 AM | Thermo Fisher Scientific | Cat# R1244 |
| Lipofectamine™ 3000 Transfection Reagent | Thermo Fisher Scientific | Cat# L3000001 |
| HitransG P | Gennechem | Cat# REVG005 |
| Recombinant Human IL-2 | PeptoTech | Cat# 200-02 |
| Recombinant Murine IL-2 | PeptoTech | Cat# 212-12 |
| Nunc™ Polycarbonate Cell Culture Inserts in Multi-Well Plates | Thermo Fisher Scientific | Cat# 140620 |
| Lymphocyte Separation Medium (Human) | Solarbio | Cat# P8610 |
| Mito-TEMPO | MCE | Cat# HY-112879 |
| OSMI-1 | Sigma Aldrich | Cat# SML1621 |
| Santacruzamate A | Selleckchem | Cat# S7595 |
| Liraglutide | MCE | Cat# HY-P0014 |

Critical commercial assays

| | | |
|-------------------------|--------------------------|------------|
| ATP Assay Kit | beyotime | Cat#S0026 |
| Pierce Crosslink IP Kit | Thermo Fisher Scientific | Cat# 26147 |

(Continued on next page)

Continued

| REAGENT or RESOURCE | SOURCE | IDENTIFIER |
|---|-----------------|------------------|
| Annexin V-FITC Apoptosis Detection Kit | beyotime | Cat# C1062S |
| MPTP Assay Kit | beyotime | Cat# C2009S |
| Dual Luciferase Reporter Gene Assay Kit | beyotime | Cat# RG027 |
| ChIP Assay Kit | beyotime | Cat# P2078 |
| Mitochondrial membrane potential assay kit with JC-1 | beyotime | Cat# C2006 |
| One Step TUNEL Apoptosis Assay Kit | beyotime | Cat# C1089 |
| BCA Protein Assay Kit | beyotime | Cat# P0011 |
| CD4 ⁺ CD25 ⁺ Regulatory T Cell Isolation Kit, mouse | Miltenyi Biotec | Cat# 130-091-041 |
| CD4 ⁺ CD25 ⁺ CD127 ^{dim/-} Regulatory T Cell Isolation Kit II, human | Miltenyi Biotec | Cat# 130-094-775 |
| Treg Expansion Kit, human | Miltenyi Biotec | Cat# 130-095-345 |
| Treg Expansion Kit, mouse | Miltenyi Biotec | Cat# 130-095-925 |

Experimental models: Cell lines

| | | |
|--|------------|-----|
| Mouse CD4 ⁺ CD25 ⁺ Treg cells | This Paper | N/A |
| Human CD4 ⁺ CD25 ⁺ CD127 ^{dim/-} Treg cells | This Paper | N/A |
| Primary microglia | This Paper | N/A |
| Primary murine hippocampal neurons | This Paper | N/A |

Experimental models: Organisms/strains

| | | |
|--|--------------------|-------------------------------------|
| Mouse: BKS.Cg-Dock7 ^m +/- Lepr ^{db} /J | Jackson Laboratory | Cat# 000642 ; RRID: IMSR_JAX:000642 |
| Mouse: Foxp3 ^{eGFP-Cre-ERT2} | This Paper | NA |
| Mouse: GLP1R ^{fl/fl} | This Paper | NA |
| Mouse: Rosa26 ^{NCLX} | This Paper | NA |

Oligonucleotides

| | | |
|--|--|---------------|
| GLP-1R siRNA and shRNA Plasmids (m) | Santa Cruz Biotechnology | Cat# sc-45764 |
| SP1 siRNA and shRNA Plasmids (h) | Santa Cruz Biotechnology | Cat# sc-29487 |
| OGT siRNA and shRNA Plasmids (h) | Santa Cruz Biotechnology | Cat# sc-40780 |
| mouse OGT siRNA 5'-AGGGAACUAGAUACAUGCUU-3' | This paper | N/A |
| Human OGA siRNA 5'-ACTCATCCCACGGTTAAAA-3' | This paper | N/A |
| LV-NCLX | This paper | N/A |
| LV-OGT | This paper | N/A |
| LV-CON | This paper | N/A |
| Mouse GAPDH qPCR F: 5'-CAGGAGGCATTGCTGATGAT -3' R: 5'-GAAGGCTGGGGCTCATTT -3' | Wuhan Jinkairui biological engineering co. | N/A |
| Human GAPDH qPCR F: 5'-GAAGGTGAAGTCCGGAGTC -3' R: 5'-GAAGATGGTATGGGATTTTC -3' | Wuhan Jinkairui biological engineering co. | N/A |
| Mouse mt-cytb qPCR F: 5'-CTAATCCACTAA ACACCCCACC-3' R: 5'-GGCTTCGTTGCTTTGAGGTAT-3' | Wuhan Jinkairui biological engineering co. | N/A |
| Human MT-CYTB qPCR F: 5'-ATCACTCGAGACGTAAATTATGGCT-3' R: 5'-TGAAGTAGGTCTGTCCCAATGTATG-3' | Wuhan Jinkairui biological engineering co. | N/A |

(Continued on next page)

Continued

| REAGENT or RESOURCE | SOURCE | IDENTIFIER |
|--|--|---|
| Mouse mt-COI qPCR F: 5'-TCAGGAATACCACGACGCTAC-3' R: 5'-GAGGGCAGCCATGAAGTCAT-3' | Wuhan Jinkairui biological engineering co. | N/A |
| Human MT-COI qPCR F: 5'-GACGTAGACACACGAGCATATTTCA-3' R: 5'-AGGACATAGTGGAAGTGAGCTACAAC-3' | Wuhan Jinkairui biological engineering co. | N/A |
| Mouse NCLX qPCR F: 5'-GGAGACCCATCCACAAAA-3' R: 5'-AGCAGAAGATGCCCTCAA-3' | Wuhan Jinkairui biological engineering co. | N/A |
| Human NCLX qPCR F: 5'-CAGAAAGGGAAGTGGAGAGTAAG-3' R: 5'-GCCATTAGCAGCACACAAAG-3' | Wuhan Jinkairui biological engineering co. | N/A |
| Software and algorithms | | |
| GraphPad Prism 9.0 | GraphPad | https://www.graphpad.com/scientific-software/prism/ |
| GEPIA | GEPIA | http://gepia.cancer-pku.cn/detail.php?clicktag=correlation### |
| IBM SPSS Statistics 24 | IBM | https://www.ibm.com/support/pages/downloading-ibm-spss-statistics-24 |
| PROMO | ALGGEN | http://alngen.lsi.upc.es/cgi-bin/promo_v3/promo/promoinit.cgi?dirDB=TF_8.3 |
| FlowJo v10 | FlowJo | https://www.flowjo.com/ |
| YinOYang 1.2 | YinOYang | https://services.healthtech.dtu.dk/service.php?YinOYang-1.2 |
| NetOGlyc 4.0 | NetOGlyc | https://services.healthtech.dtu.dk/service.php?NetOGlyc-4.0 |
| O-GlcNAc Database (v1.2) | O-GlcNAc | https://www.oglcnac.mcw.edu/ |

RESOURCE AVAILABILITY

Lead contact

Further information and requests for resources and reagents should be directed to and will be fulfilled by the Lead Contact, Tianpeng Zheng (w19831120@126.com).

Materials availability

This study did not generate new unique reagents.

Data and code availability

Data reported in this paper will be shared by the [lead contact](#) upon request. This paper does not report original code. Any additional information required to reanalyze the data reported in this paper is available from the [lead contact](#) upon request.

EXPERIMENTAL MODEL AND SUBJECT DETAILS

Mice

To generate db/db $Foxp3^{Cre-ERT2}$ $GLP1R^{fl/fl}$ mice, db/m mice were mated with $GLP1R^{fl/+}$ mice to obtain db/m $GLP1R^{fl/fl}$ mice, which were then mated with $Foxp3^{Cre-ERT2}$ mice. db/m $Rosa26^{NCLX}$ mice were obtained by breeding $Rosa26^{NCLX}$ mice with db/m mice, and db/db $Foxp3^{Cre-ERT2}$ $Rosa26^{NCLX}$ mice were produced by further breeding between db/m $Rosa26^{NCLX}$ mice and $Foxp3^{Cre-ERT2}$ mice. All mice were housed under standard laboratory conditions (12hr light/dark cycle, 07:00 to 19:00 light on) and temperature (23-24°C) with *ad libitum* access to water and standard laboratory chow diet. To activate Cre LoxP recombination, 8-week-old mice were fed for 5 weeks with a diet containing tamoxifen (400 mg tamoxifen/kg chow, Teklad, TD.130860). The efficiency of overexpression or knockdown was examined by quantitative reverse transcription-PCR (qRT-PCR) or immunoblotting assays after the final tamoxifen treatment. To further test whether GLP-1 receptor agonists could improve cognitive function in diabetes, 4 months old db/db mice were given liraglutide at a dose of 246.7 µg/kg/day by subcutaneous injection

for 4 weeks, while the age matched control groups were administered the same volume of vehicle. The dose of liraglutide (246.7 $\mu\text{g}/\text{kg}/\text{day}$) was equivalent to the common human dose (20 $\mu\text{g}/\text{kg}/\text{day}$) normalized to body surface area across species.³⁸ Five-month-old mice from different groups were subjected to Morris water maze and active avoidance memory test. All animal experiments were performed in accordance with guidelines approved by the Animal Care and Experimentation Committee at Guilin Medical University.

Human samples

The participants were enrolled from May 2021 to March 2022 at the Department of Endocrinology and Metabolism of the Second Affiliated Hospital of Guilin Medical University. A total of 100 participants aged 60 years or older were enrolled, of which 30 nondiabetic subjects, 36 newly diagnosed type 2 diabetic patients without cognitive dysfunction and 34 type 2 diabetic patients with mild cognitive impairment. The mild cognitive impairment diagnoses were based on the criteria recommended by the National Institute on Aging-Alzheimer's Association (NIA-AA) workgroups. The exclusion criteria were as follows: (1) presence of secondary diabetes; acute diabetic complications, inflammatory diseases, infectious diseases; autoimmune disease; hypothyroidism, hypertensive crisis, malignancy, heart, liver, kidney, and respiratory failure; (2) use of GLP-1 receptor agonists or DPP4 activity inhibitors at any time within 12 months before the enrollment; (3) participants with missing or incomplete data. To further test whether GLP-1 receptor agonists could improve cognitive function in type 2 diabetes, type 2 diabetes patients with mild cognitive impairment were subcutaneous injected with liraglutide for 3 months. Starting dose was 0.6 mg/day, the dose was increased to 1.2 mg/day for the second week, and the final dose was 1.8 mg/day. For each participant, cognitive test and peripheral blood samples collection were performed at baseline (prior to first liraglutide injection) and at end of the study. The Ethical Committee of the Second Affiliated Hospital of Guilin Medical University reviewed and approved the study. The written informed consent was obtained from each participant prior to sample collection.

Cell isolation and culture

Primary microglia were isolated from mixed primary glial cultures that were obtained from the hippocampus of E18 mouse embryos. Briefly, hippocampus was dissected from the brain after removing the meninges and blood vessels. The dissociated cells were plated onto 0.01% Poly-L-lysine-coated T-25 culture flasks filled with culture media (DMEM containing 10% heat-inactivated fetal bovine serum and 1% penicillin/streptomycin), and cultivated at 37°C with 5% CO₂. Primary microglia were isolated from mouse mixed glial cultures using the shaking method. Cultures of hippocampal neurons were prepared as described previously.^{4,39} Briefly, the hippocampus was extracted from the brain and subsequently sectioned into 1 mm³ fragments using a blade. The shredded tissue was then subjected to trypsin digestion at a concentration of 0.125% and incubated at 37°C for 10 minutes. Following enzymatic digestion, the reaction was terminated by 10% fetal bovine serum (FBS). The resulting tissue supernatant was collected and centrifuged at 1000 g for 5 minutes. The cell pellet underwent a cold PBS wash and was subsequently suspended in Neurobasal A medium supplemented with 2% B27 (Invitrogen) and glutamine (0.5 mM, Invitrogen). Finally, neurons were plated on poly-L-lysine-coated six-well plates (Sigma-Aldrich) and cultured at 37°C with 5% CO₂.

Mouse CD4⁺ CD25⁺ Treg cells were isolated from the lymph nodes and spleen of mice in different groups using a Treg cell isolation kit (Miltenyi Biotec 130-091-041) according to the manufacturer's protocol. Human Treg cells were isolated using the CD4⁺CD25⁺CD127^{dim/-}Regulatory T Cell Isolation Kit II (Miltenyi Biotec 130-094-775). The purity of human and mouse CD4⁺CD25⁺Foxp3⁺ Treg cells were assessed by flow cytometry and cells were used when purity exceeded 95%. Human and mouse Treg cells were expanded according to the protocol provided by the Treg Expansion Kit (Miltenyi Biotec 130-095-345; Miltenyi Biotec 130-095-925).

For *in vitro* experiments in Treg cells, high glucose was engendered by raising the glucose 25mM over ambient conditions. The selection of this glucose level was based on the findings of preliminary studies, which revealed a significant dose-response relationship between glucose levels and its effects on Treg cells. Additionally, this level was chosen to emulate moderate-to-severe type 2 diabetes, as it corresponds to a blood glucose range of 450mg/dl.

METHOD DETAILS

Gene silencing and overexpression

The lentivirus constructs were used to stably overexpress target proteins in Treg cells according to the manufacturer's recommended protocol. After 72 h, cells were tested for overexpression efficiency. For *in vitro* siRNA-mediated knockdown, Treg cells were transfected with either the targeting or control siRNA using Lipofectamine 3000. Cells were incubated 72 h prior to assessing knockdown efficiency via immunoblot analysis.

Immunoblot and Co-immunoprecipitation analysis

Cell lysates were prepared in RIPA buffer supplemented with proteinase and phosphatase inhibitors. Proteins were separated by 10% SDS-PAGE and transferred to a polyvinylidene difluoride membrane. Membranes were blocked for 15 min at room temperature in QuickBlock™ Blocking Buffer and were incubated overnight at 4°C with the specific primary antibodies. After 3 washes of 5 min in TBST, membranes were incubated with secondary antibodies diluted in QuickBlock™ Secondary Antibody Dilution Buffer for 2 h at room temperature. After 3 washes of 5 min in TBST, membranes were incubated with enhanced chemiluminescence (ECL) reagent.

For COIP analysis, HEK293T and Treg cells were transfected with indicated expression vectors. 72 h after transfection, cells were lysed in IP lysis buffer with proteinase and phosphatase inhibitors. Indicated antibodies and protein A/G agarose beads were added and incubated with the lysates. After washing with IP buffer, the precipitated proteins were eluted from the beads by boiling in SDS loading buffer for 5 min.

Chromatin immunoprecipitation

Treg cells were cross-linked using 1% formaldehyde for 10 min at 37°C. Cross-linked cells were sonicated according to the manufacturer's protocol. Thereafter, DNA-protein complexes in the lysates were immunoprecipitated using indicated antibodies or control normal IgG. After precipitation of the immunocomplex with protein A/G agarose, isolated DNAs were quantified by qPCR.

RNA preparation and quantitative PCR

Total RNA was isolated from Treg cells using TRIzol reagent (Invitrogen). The mRNA was then reverse transcribed into cDNA using FastKing RT Kit (TianGen). Quantitative real-time PCR analysis was performed with specific primers, cDNA and SYBR Green PCR Master Mix (Monad). Relative mRNA expression was determined using the $2^{-\Delta\Delta CT}$ method and normalized to GAPDH mRNA levels.

Immunofluorescence

Treg cells were fixed in 4% paraformaldehyde at room temperature for 30 min. After three washes with PBS, the cells were blocked with QuickBlock™ Blocking Buffer (Beyotime) for 1h. Afterwards, Treg cells were incubated overnight at 4°C with the indicated primary antibodies and then incubated with secondary antibody for 2 h at room temperature. DAPI (5ug/ml) was used to counterstain cell nuclei and fluorescence images were obtained using a fluorescence microscope (Olympus).

ATP measurement

The ATP level in Treg cells was measured using the ATP Assay Kit (Beyotime). Briefly, Treg cells were lysed with ATP sample buffer and cell lysates were added to the 96-well plate. Another standard reaction buffer containing luciferase and luciferin were added and incubated 30 min at room temperature. The luminescence was measured by a multifunctional microplate reader.

Detection of reactive oxygen species (ROS)

Mitochondrial ROS levels in Treg cells were measured by MitoSOX™ Red (Thermo Fisher Scientific). Briefly, Treg cells were incubated with MitoSOX™ reagent working solution for 10 min at 37°C and washed with HBSS to remove free MitoSOX. The mean fluorescence intensity was measured using a flow cytometer, and the data were analyzed using FlowJo (v10) software.

Apoptosis assays

For apoptosis assays, Treg cells were stained using a Annexin V-FITC apoptosis detection kit as per manufacturer's instructions. Samples were analyzed using flow cytometer.

Mitochondrial Ca²⁺ Measurement

To measure mitochondrial Ca²⁺, Treg cells were washed with HBSS, followed by incubation with Rhod-2 AM and Pluronic F-127 for 30 min at 37°C, and then analyzed by a flow cytometer.

MPTP

Mitochondrial permeability transition pore opening in Treg cells was monitored using the mitochondrial Transition Pore Assay Kit according to the manufacturer's protocol. Briefly, Treg cells were incubated with fluorescent dye calcein-AM and CoCl₂ in HBSS for 30 min at 37°C. Calcein-loaded cells were then washed with HBSS and fluorescence pictures were taken using a fluorescent microscope.

Mitochondrial membrane potential measurement

Mitochondrial Membrane Potential Assay Kit was used to assess mitochondrial membrane potential. Briefly, Treg cells were collected and incubated with JC1 dye for 20 min at 37°C. The fluorescence of JC-1 was measured by a flow cytometer.

Transmission electron microscopy (TEM)

Mitochondrial structure was examined by transmission electron microscopy. Treg cells were fixed in 2.5% glutaraldehyde at 4°C overnight, post-fixed with 1% osmium tetroxide for 2 h at room temperature. Subsequently, cells were washed, dehydrated, and embedded in resin according to standard procedures. Embedded samples were sectioned at 70-nm thickness, and stained with uranium acetate/lead citrate. Images were captured using a Hitachi-HT7700 electron microscopy (Hitachi).

Morris water maze

Morris water maze test was performed as previously described.^{4,39} For training trials, the platform was submerged below the water surface. Mice were trained with 4 trials each day for five consecutive days to find the hidden platform. The probe trial was conducted on the sixth day, when each mouse was allowed 60 seconds to search the position of removed platform. All parameters were recorded using a Video Tracker software.

Active avoidance memory test

The active avoidance memory test was used to assess spatial learning and memory as previously reported.^{4,39} The active avoidance test was controlled by a computer program that generated the electric shock, sound, and light. During the training session, each mouse was given two trials for 3 consecutive days. The avoidance responses of the mice were recorded automatically.

Bioinformatics analysis

Transcription factors that could bind to the promoter region of NCLX were predicted by PROMO (ALGGEN, http://alggen.lsi.upc.es/cgi-bin/promo_v3/promo/promoinit.cgi?dirDB=TF_8.3). The correlation analysis of gene expression was performed using the Gene Expression Profiling Interactive Analysis (GEPIA, <http://gepia.cancer-pku.cn/>). O-glycosylation sites were predicted using YinOYang 1.2, NetOGlyc 4.0 and the O-GlcNAc Database (v1.2).

QUANTIFICATION AND STATISTICAL ANALYSIS

All data were analyzed using Prism version 9.0 software (GraphPad) and expressed as mean \pm standard error of mean (SEM) or median (interquartile range). Kolmogorov-Smirnov test was used to evaluate the normality of the data distribution. Comparisons between two groups were performed using two-tailed Student's t test for normally distributed data and Mann-Whitney rank sum test for non-normally distributed data. One-way ANOVA followed by post hoc Tukey's test was used to compare differences between multiple groups. The statistical differences were analyzed by unpaired student t tests when comparing two groups, or by a one-way ANOVA when comparing more than two groups. All p-values below 0.05 were accepted as statistically significant. In figures, asterisks are used to indicate statistical significance (* P<0.05, ** P<0.01, *** P<0.001).